Auto Rickshaw Impacts with Pedestrians: A Computational Analysis of Post-Collision Kinematics and Injury Mechanics

A. J. Al-Graitti, G. A. Khalid, P. Berthelson, A. Mason-Jones, R. Prabhu, M. D. Jones

Abstract—Motor vehicle related pedestrian road traffic collisions are a major road safety challenge, since they are a leading cause of death and serious injury worldwide, contributing to a third of the global disease burden. The auto rickshaw, which is a common form of urban transport in many developing countries, plays a major transport role, both as a vehicle for hire and for private use. The most common auto rickshaws are quite unlike 'typical' four-wheel motor vehicle, being typically characterised by three wheels, a non-tilting sheet-metal body or open frame construction, a canvas roof and side curtains, a small drivers' cabin, handlebar controls and a passenger space at the rear. Given the propensity, in developing countries, for auto rickshaws to be used in mixed cityscapes, where pedestrians and vehicles share the roadway, the potential for auto rickshaw impacts with pedestrians is relatively high. Whilst auto rickshaws are used in some Western countries, their limited number and spatial separation from pedestrian walkways, as a result of city planning, has not resulted in significant accident statistics. Thus, auto rickshaws have not been subject to the vehicle impact related pedestrian crash kinematic analyses and/or injury mechanics assessment, typically associated with motor vehicle development in Western Europe, North America and Japan. This study presents a parametric analysis of auto rickshaw related pedestrian impacts by computational simulation, using a Finite Element model of an auto rickshaw and an LS-DYNA 50th percentile male Hybrid III Anthropometric Test Device (dummy). Parametric variables include auto rickshaw impact velocity, auto rickshaw impact region (front, centre or offset) and relative pedestrian impact position (front, side and rear). The output data of each impact simulation was correlated against reported injury metrics, Head Injury Criterion (front, side and rear), Neck injury Criterion (front, side and rear), Abbreviated Injury Scale and reported risk level and adds greater understanding to the issue of auto rickshaw related pedestrian injury risk. The parametric analyses suggest that pedestrians are subject to a relatively high risk of injury during impacts with an auto rickshaw at velocities of 20 km/h or greater, which during some of the impact simulations may even risk fatalities. The present study provides valuable evidence for informing a series of recommendations and guidelines for making the auto rickshaw safer during collisions with pedestrians. Whilst it is acknowledged that the present research findings are based in the field of safety engineering and may over represent injury risk, compared to "Real World" accidents, many of the simulated interactions produced injury response values significantly greater than current threshold curves and thus, justify their inclusion in the study. To reduce the injury risk level and increase the safety of the auto rickshaw, there should be a reduction in the velocity of the auto rickshaw and, or, consideration of engineering solutions, such as retro fitting injury mitigation technologies to those auto rickshaw contact regions which are the subject of the greatest risk of producing pedestrian injury.

Keywords—Auto Rickshaw, finite element analysis, injury risk level, LS-DYNA, pedestrian impact.

I. INTRODUCTION

MOTOR vehicle related pedestrian road traffic collisions are a major road safety challenge, which according to the World Health Organization produce almost a quarter of all road traffic related deaths [1].

Accidents in developing countries can be 70 times more likely to occur than in developed countries and the vast majority of road accident fatalities are vulnerable road users, such as pedestrians [2]. Analysis of accident data in China between 2000 and 2007 indicates that 25% of fatalities were caused by road traffic accidents [3]. Whilst in Saudi Arabia, the annual traffic statistics in 1999 showed that road accidents caused almost 6000 serious pedestrian injuries and 1000 deaths [4]. In Africa, pedestrian fatality is a major issue, with road traffic accidents accounting for an estimated 39% of all deaths in Tanzania and 75% in Cote d'Ivoire [5]. In Bangladesh, pedestrian accidents with auto rickshaw, buses, trucks and tractors had a higher fatality risk than impacts with cars [6].

Whilst many vehicle related studies have been focused on the kinematic behaviour of pedestrian-vehicle impacts [7]-[15], the auto rickshaw, a common form of urban transport in many developing countries, has received relatively little consideration [16], [17]. Collision dynamics and injury have not been extensively and comprehensively studied for pedestrian-auto rickshaw collisions. The auto rickshaw typically has three wheels and a frontal geometry consisting a mudguard with an attached headlamp, an upright body and windscreen, a canvas roof and a small cabin, with a maximum velocity of 55 km/h [18].

The incidents of pedestrian collisions with auto rickshaws are high in developing countries as a consequence of the mixed sharing of urban roads [19]-[22]. In contrast, in those European countries, which use auto rickshaws, there are a

A. J. Al-Graitti is a PhD researcher at Cardiff School of Engineering, Cardiff University, UK who is sponsored by the Higher Committee for Educational Development (HCED) Iraq (e-mail: al-graittiaj@cardiff.ac.uk).

G. A. Khalid is a researcher at Cardiff School of Engineering, Cardiff University, UK and a lecturer at the College of Electrical and Electronic Engineering Techniques, Middle Technical University, Baghdad, Iraq (e-mail: KhalidGA@cardiff.ac.uk).

*M. D. Jones and A. Mason-Jones are lecturers at Cardiff School of Engineering, Cardiff University, Cardiff, UK (*corresponding author, e-mail: jonesmd1@cardiff.ac.uk, mason-jonesa@cardiff.ac.uk).

R. Prabhu is an Assistant Professor and P. Berthelson is a M.Sc. student at the Department of Agricultural and Biological Engineering and the Center for Advanced Vehicular Systems at Mississippi State University, Mississippi, USA (e-mail: rprabhu@abe.msstate.edu, prb99@msstate.edu).

comparatively small number of accidents, since, as a result of city planning, vehicles and pedestrians are generally separated. Improving the urban infrastructure, to separate pedestrians from vehicles, requires very significant capital investment. Thus, a more realisable aim is to engineer an improvement in the auto rickshaw to improve pedestrian collision kinematics. Vehicle-pedestrian collision accident data shows that head and neck injury are the most common injury types and can lead to life changing injuries, disability or even death [3], [23]-[26]. The societal cost resulting from head and neck injuries can be considerable as services need to be provided on a long term, or even life-long, basis [27].

Pedestrian road accident investigations have determined that the vast majority of pedestrian impact injuries are associated with impact velocities of between 25 km/h and 55 km/h [28], [29]. Many studies concur that the impact velocity is a key determinant of injury severity in pedestrian-collision [30]-[40]. Therefore, many regulations have been established worldwide to control vehicle driving speed in urban areas. In the UK, for example, it was legislated that between 32 km/h and 48 km/h limits be applied in urban environments [41]. In addition, during vehicle safety tests, 35 km/h and 40km/h were recommended by the Global Technical Regulations (GTR) and European New Car Safety Assessment Program (Euro-NCAP), respectively [42], [43].

Road traffic accident data shows that 14% of pedestrians are impacted on their anterior face, 8% on their posterior face, almost 73% are impacted laterally and 5% were impacted under unknown conditions [44]. In addition, 6% of the pedestrians impacted were standing with legs together, 5% were impacted with legs apart laterally, 65% were found to be in a gait stance at the time of collision and 24% were in an unknown stance [45].

Whilst many researchers have studied pedestrian head injuries for different vehicle front-end geometries, there are many additional auto rickshaw specific parameters which might uniquely affect pedestrian kinematics and injury mechanisms, such as, the unique frontal geometry, impact position, vehicle contact surface region and impact velocity. In addition, neck injury has not been comprehensively evaluated.

The purpose of this present study was to investigate the influence of impact velocity, vehicle contact region and impact position on the kinematic response and injury risk of the pedestrian head and neck. The total pedestrian kinematics and injury mechanism of the head and neck were analysed for different collision scenarios, using different injury criteria, risk levels and different injury thresholds.

II. METHOD AND MATERIALS

A parametric study was conducted, investigating the variables of: impact velocity, pedestrian front, side and rear impact orientation in the standing and walking positions and the vehicle contact surface region (centreline and offset). Vehicle frontal geometry and impact compliance property studies were conducted with a validated FE pedestrian dummy model [46]. The effect of impact velocity was examined with 10 different impact velocities with an auto rickshaw,

according to the frequency of involvement in real world accidents, in terms of calculated injury parameters. The injury parameters were compared in terms of head injury criteria (HIC) and neck injury criteria (N_{ij} and N_{km}). The Abbreviated Injury Scale (AIS) and injury thresholds were compared with the risk level to indicate the threat to life.

A. Model Setup

The 50th percentile Hybrid III adult male pedestrian FE dummy model was utilised in this study. The dummy standing height and weight are approximately 1680 mm and 78.6 kg, respectively.

B. Vehicle Model

The three-wheel vehicle geometry was meshed by ANSA-software using linear quadrilateral and triangular elements. The overall vehicle mesh quality was controlled in the modelling process shown in Table I. The total mass of the auto-rickshaw, including the driver, was 373 kg, while the centre of gravity and the moment of inertia were measured by LS-DYNA software. To minimise computational run time the rear vehicle components were simplified, such that only one element was generated to represent the same mass, centre of gravity and moment of inertia of the simplified parts to make the model masses the same as the original simplified ones. The front of the auto rickshaw model consists of a mudguard, headlamp, frontal sheet plate, sheet plate edge, windscreen, windscreen frame and one tyre, as shown in Fig. 1. All of the vehicle components were jointed together by using relevant constraint types within the FE software, LS-DYNA, to decrease the motion space.

TABLE I
ELEMENT QUALITY CONTROL PARAMETERS

Quality Parameter	Allowable Min/Max
Minimum side length	5.0
Maximum side length	100
Maximum aspect ratio	5.0
Minimum quadrilateral internal angle	45.0
Maximum quadrilateral internal angle	145.0
Minimum triangular internal angle	15.0
Maximum triangular internal angle	120.0
Maximum warp angle	15.0
% of triangles	5.0

Fig. 1 FE Model of the front of the auto rickshaw

C. Material Properties

The vehicle component materials were selected by LS-

DYNA material library. The tyre was modelled by MAT_ELASTIC. While the windscreen and vehicle structure were modelled by MAT_PIECEWISE_LINEAR_PLASTICITY. The material mechanical properties and shell thicknesses of the vehicle parts are shown in Tables II and III.

TABLE II
MATERIAL MECHANICAL PROPERTIES OF THE MODEL VEHICLE COMPONENTS

Vehicle item	Mass Density (kg/mm³)	Young's Modulus (GPa)	Poisson's Ratio	Yield Stress (GPa)	References
Tyre	1.700e-006	24.61	0.32	-	[47], [48]
Windscreen	2.500e-006	76.00	0.30	0.13	[49]-[51]
Vehicle Structure	7.890e-006	210.0	0.30	250	[49]

TABLE III
THICKNESS OF THE VEHICLE COMPONENTS

Vehicle item	Thicknesses (mm)
Tyre	3 [52]
Windscreen	5.8 [53]-[55]
Vehicle structure	1.2-2 [56]

D. Setup of the Simulations

LS-DYNA software was utilised for all of the collision analyses, 60 simulations were conducted for one auto rickshaw-pedestrian collision with impact velocities of 5 km/h, 10 km/h, 15 km/h, 20 km/h, 25 km/h, 30 km/h, 32 km/h, 35 km/h, 40 km/h and 48 km/h. The pedestrian model was positioned in contact with two main vehicle contact regions, at the centreline and 42 cm offset from the vehicle centreline, with three major impact positions. Including front (face-to-face with the vehicle), rear (back-to-face) and in a walking posture facing laterally with the right leg forward (without a walking speed), and the left arm positioned backward to cover the whole possible impact scenarios, see Fig. 2. The contact between the auto rickshaw and the dummy was defined by AUTOMATIC_SURFACE_TO_SURFACE [57]. AUTOMATIC_GENERAL was utilised to define the interaction between the auto rickshaw tyre and the ground along the moving path [58]. The contact friction coefficient, between the pedestrian dummy parts and rickshaw was 0.65, and the coefficient between the dummy shoes and ground was 0.7 [3], [57], [59], shown in Fig. 3. In addition, LS-DYNA software was used to collect the post collision output data. To reduce the uncertainty in time shifts, when comparing the electronic data films, a Butterworth pre-filter with a frequency of 180 of c/s (Hz) was used to collect the head and neck loading and criteria, as recommended by the National Highway Traffic Safety Administration (NHTSA) agency [60], [61].
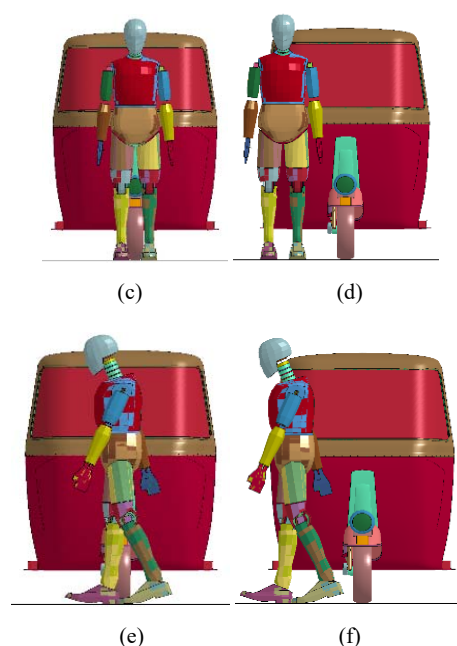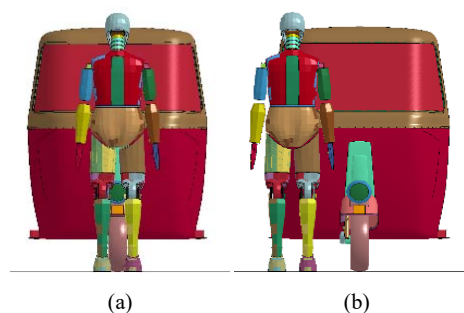

Fig. 2 Auto rickshaw-pedestrian impact simulations at different positions and contact angles;(a) Frontal impact to front of head at the centreline of the vehicle; (b) Frontal impact to front of head, 42 cm offset from vehicle centreline; (c) Rear impact to back of head at centreline of the vehicle; (d) Rear impact to back of head, 42 cm offset from vehicle centreline; (e) Side impact during walking to side of head at centreline of vehicle; (f) Side impact during walking to side of head, 42 cm offset from vehicle centreline
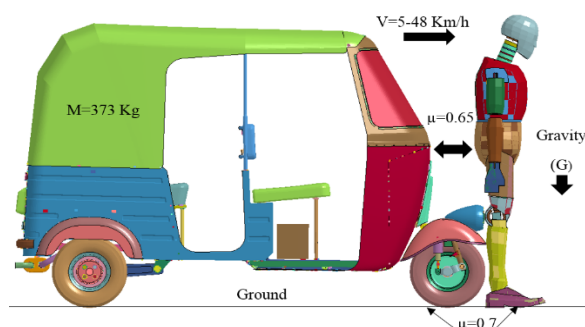

Fig. 3 Vehicle-pedestrian impact simulation

E. Selected Injury Parameters

The pedestrian injury risks were evaluated in terms of selected injury parameters and tolerance levels, see Tables IV

and VII. The Head Injury Criterion (HIC_{15}) and the Neck Injury Criterion (N_{ij} and N_{km}) were used to assess the risk of pedestrian head and upper neck injury.

1. Head Injury and Risk Level

Head injury risk was calculated by the HIC, determined from the correlation between resultant acceleration of the head and the time, such as Fig. 16 in the appendix.

$$HIC = \left\{ \frac{1}{t_2 - t_1} \int_{t_1}^{t_2} a \ dt \cdot \right\}^{2.5} (t_2 - t_1)_{max} \qquad (1)$$

where a, is the resultant linear acceleration measured at the head centre of gravity in units of gravity; t_1 and t_2 are the two time instants during the collision, describing an interval between the starting and the end of the recording time - period, identifying the maximum value of HIC , i.e. ($t_2 - t_1 \leq 15$ ms) [62].

The HIC injury threshold is 1000 for the front and rear impact tests [63]-[65] and 800 for the side impacts [57]. The thresholds in Table IV indicate an 18% probability of sustaining a severe head injury (AIS+4) [63], such as brain haemorrhage and/or skull fracture [63]-[67].

TABLE IV
HEAD INJURY THRESHOLDS

Impact Position	Injury Threshold
Front	1000 [63]-[65]
Rear	1000 [65]
Side	800 [68]-[70]

2. Upper Neck Injury and Risk Level

The initial neck injury research: threshold, tolerance to impact, biomechanical materials, strengths and injury pathways were obtained by standardised Anthropomorphic Test Devices (ATDs) to provide a criterion for predicting injury risk to persons with varying anthropometric characteristics for various automotive crash and restraint systems [60], [71]-[73].

NHTSA established a neck injury criterion with four neck loading types and critical limits for both front and rear impacts [60], [74]. Frontal impacts are an important measure for frontal collision related neck injury. Upper neck axial forces and moments, measured at the occipital condyles, in the appendix, see Tables XIII-XVI used to calculate the neck injury criteria (N_{ij}), and see Tables XVII and XVIII, which can be compared against tolerance levels for axial force and bending moments. The formulae used to calculate the N_{ij}:

$$N_{ij} = \frac{F_z}{F_{int}} + \frac{M_y}{M_{int}} \qquad (2)$$

F_Z represents the maximum axial force (tension/ compression) and M_y represents the maximum flexion (forward)extension (rearward) bending moment [75]. Four different load cases are associated with the neck injury criterion (N_{ij}), N_{te}, N_{tf} N_{ce} and N_{cf}, where N_{te} represents tension-extension, N_{tf} represents tension-flexion, N_{ce} represents compression-extension and N_{cf} represents compression-flexion for both load and moment. The index "int" gives a critical intercept value for both the load and moment of the Hybrid III male dummy as shown in Table V. The intercept values of the Hybrid III are calculated from the output wave signal of both the load and moment, such as Figs. 17 and 18, shown in the appendices.

TABLE V
INTERCEPT LOAD VALUES FOR THE 50TH PERCENTILE HYBRID III MALE DUMMY FOR FRONT IMPACT

Load case	Values [60]
Extension	-135 N.m.
Flexion	+310 N.m.
Tension force	+6806 N.
Compression force	-6160 N.

Rear impacts, are represented by N_{km} force and moment are similarly measured at the occipital condyles, see Tables XIX-XXII in the appendices, and is based on the tolerance levels for shear force and bending moment. The formula utilised to calculate the N_{km} is as:

$$N_{km} = \frac{F_x}{F_{int}} + \frac{M_y}{M_{int}} \qquad (3)$$

where F_x represents the maximum shear force (anterior/ posterior) and M_y represents the maximum flexion (forward)/ extension (rearward) bending moment. There are four possible load cases associated with N_{km}: the N_{fa}, N_{ep}, N_{fp}, and N_{ea} , see Tables XXIII and XXIV in the appendices, where N_{fa} represents flexion-anterior, N_{ep} represents extension-posterior, N_{fp} represents flexion-posterior and N_{ea} represents extension-anterior. The index "int" gives a critical intercept value for both the load and moment, as shown in Table VI. The intercept values of the Hybrid III are calculated from the output wave signal of both the load and moment, such as Figs. 18 and 19, shown in the appendices

TABLE VI
INTERCEPT LOAD VALUES FOR THE 50TH PERCENTILE HYBRID III MALE DUMMY FOR REAR IMPACT

Load case	Values [70], [76]
Extension	47.5 N.m
Flexion	+88.1 N.m
Shear force	±845 N

TABLE VII
NECK INJURY THRESHOLDS

Impact Position	Injury Threshold
Front N_{ij}	1 [74]
Rear N_{km}	1 [77]
Side N_{ij}	1 [78]

Both N_{ij} and N_{km}, threshold values of 1 are widely utilised for the upper neck injury assessments for the front, rear and side impact tests [74], [77], [78]. These thresholds, shown in Table VII, correspond with a 22% probability of sustaining serious neck injury (AIS+3) [74], which are associated with a risk of rupture of small blood vessels of the occipital condylar joints. An increasing N_{ij} and N_{km} are associated with ligament

rapture, damage to the spinal cord, brainstem and death [74], [79], [80].

3. The AIS with the Risk Levels

The AIS has six levels of increasing risk of 'threat to life' as: 1. is considered minor, 2. is moderate, 3. is serious, 4. is severe, 5. is critical and 6. is fatal injury [81]-[84]. The AIS was used to investigate the injury risk level of the dummy head and neck.

Severe head injury (AIS+4) was used to assess head injury risk for front, rear and side impacts using the formula [85]:

$$AIS \geq 4 = \left\{1 + e^{(5.02 - 0.00351*HIC)}\right\}^{-1} \qquad (4)$$

and serious neck injury (AIS+3) was used to assess the risk of upper neck injury for front and rear collisions using NHTSA formula [53]:

$$AIS \geq 3 = \frac{1}{1 + e^{3.227 - 1.969 N_{ij}}} \qquad (5)$$

III. RESULTS

A. Pedestrian Kinematic Response

In general, the impact contact time between the impacted pedestrian body parts and the impacting vehicle decreases with increasing impact velocity for the 10 different collision velocities. Dummy kinematics were captured for all of the collision simulations. Examples of 30 km/h impact related kinematic responses are provided for three different pedestrian impact positions against two vehicle contact regions are illustrated in Fig. 4.

All the sequences of pedestrian-vehicle interaction and contact time, during the impact simulations, are shown in Tables VIII and IX. Fig. 4 shows the kinematic response of the adult dummy impacted at 30 km/h at the auto rickshaw centreline and 42 cm offset from the centreline.

Fig. 4 (a) shows the kinematic response of impacts at the vehicle centreline for front, rear and side pedestrian impact orientations.

Frontal impact occurred between the pedestrian knees and the front head lamp. Tibial contact occurred with the mudguard, followed by the lower torso contacting the frontal vehicle edge (the windscreen frame) and the upper torso, specifically the chest, impacting with the windscreen. The head was accelerated in both the forward and vertical directions, colliding with the upper windscreen and upper part of the windscreen frame at the same time. Finally, the adult pedestrian moved in the backward direction with simple rotation towards the left side of the vehicle.

Rear impact occurred between both knees and the head lamp. Tibial contact occurred with the mudguard and the lower torso contacted the frontal vehicle edge, producing a high impact force. Right and left hands produced a glancing impact with the lower frontal sheet plate, and then the upper torso struck the windscreen. The head contacted with the upper vehicle windscreen frame. Then, the adult pedestrian moved in the forward direction, though was not rotated.

Side impact occurred between the right knee and head lamp, which produced pedestrian ankle pro and supination and a high force, concentrated at the right hand and arm, as a result of contact with the lower frontal sheet plate and frontal leading edge. In addition, the right arm pushed behind the pedestrian upper torso and the femur rotate in accordance with auto rickshaw frontal vehicle geometry. Subsequently, the upper right arm impacted with the windscreen. The dummy was then observed to vault over the auto rickshaw, such that the head struck the upper side of the windscreen frame, before rotating to the right side of the vehicle.

Fig. 4 (b) shows the kinematic response of pedestrian impacted at 42 cm offset from the vehicle centreline. Front offset impact occurred between the lower torso and the frontal offset vehicle edge producing a high force. The right femur struck at the frontal lower sheet plate, the right hand and arm were impacted by the frontal vehicle edge and the frontal lower sheet plate. Subsequently, the upper torso, specifically the chest, interacted with the windscreen, the right knee impacted with the frontal lower sheet plate and the head with the upper side of the windscreen region. Finally, the dummy rotated, and the left femur contacted with the frontal lower sheet plate and the right side of the vehicle.

TABLE VIII
THE SEQUENCE OF PEDESTRIAN-VEHICLE INTERACTION AND CONTACT TIME AT THE VEHICLE CENTRELINE

Impact Position	Vehicle Contact Region	Pedestrian Contact Region	Contact Time (ms)
Front	Front head lamp	Knees	0–20
	Mudguard	Tibia	0-35
	Front vehicle edge (windscreen frame)	Lower torso	30-75
	Windscreen	Upper torso, specifically the chest	35-75
	Upper windscreen and upper frame	Head	50-65
Rear	Front head lamp	Knees	0-17
	Mudguard	Tibia	2-47
	Frontal vehicle edge (windscreen frame)	Lower torso	27-54
	Windscreen	Upper torso	62-72
	Upper windscreen frame	Head	82-92
Side	Headlamp	Right knee	0-49
	Lower front sheet plate and front leading edge	Right hand and arm	22-27
	Windscreen	Upper right arm	52-85
	Upper side of the windscreen frame	Head	100-105

Initial offset rear impact occurred between the lower torso and the front leading edge. The left hand impacted the lower vehicle sheet plate and the left arm impacted the frontal leading edge. The left knee impacted the lower frontal sheet plate and the left tibia impacted the lower sheet plate. The dummy was subsequently rotated to the right of the vehicle, the head simultaneously impacted with the upper side corner of the windscreen and windscreen frame. No impacts occurred at the upper torso.

The initial offset side impact occurred between the right arm and the right leading edge and the right hand impacted

with the lower front sheet plate. Subsequently, the right hand twisted behind the upper torso and the whole body rotated to the right of the vehicle, such that the right femur struck the lower sheet plate. The dummy subsequently turned to face the vehicle. However, no torso or head contact occurred. Finally, the dummy rotated further to the right side of the vehicle. Thus, for all impact positions the first interaction occurred between the frontal leading edge and the lower torso and upper limbs, then impact occurred with other pedestrian body regions, as shown in Table IX. The rotational dynamic for the pedestrian was the significant kinematic response in all impact positions. However, only during the side impact was there a simple rotation about the longitudinal axis.
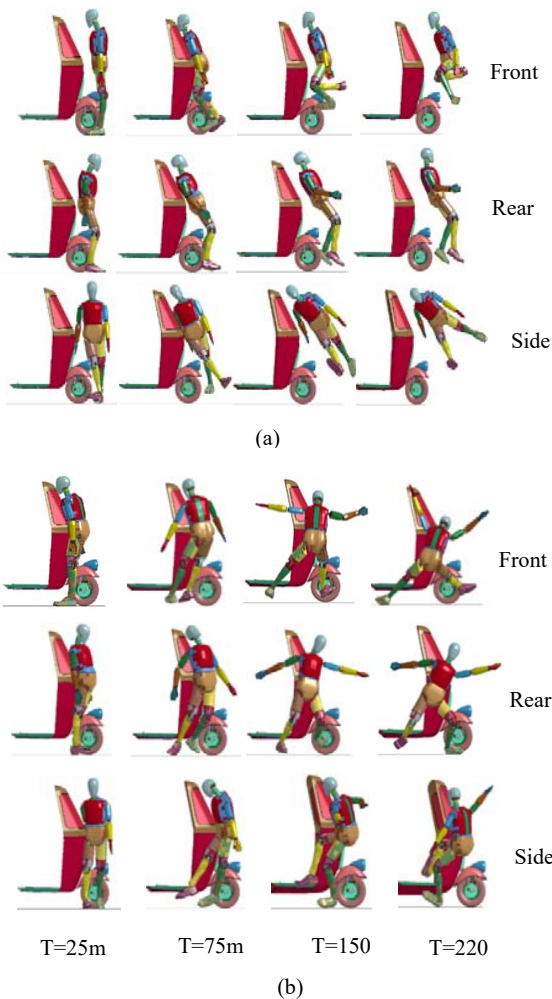

(a)

T=25m   T=75m   T=150   T=220

(b)

Fig. 4 The kinematic response of adult pedestrian dummy impacted at different vehicle regions and impact positions; (a) pedestrian impacted at the vehicle centre in front, rear and side position; (b) pedestrian impacted at 42 cm offset of the vehicle centre in front, rear and side position at 30 km/h

B. Head Contact Locations, Angles, and Time

From the impact simulations, it is established that the head contact angles vary greatly depending on impact location and vehicle contact region, see Table X. The windscreen and the

windscreen frame are the most frequently impacted, stiffest and most injurious vehicle components, as shown in Fig. 5.

TABLE IX
THE SEQUENCE OF PEDESTRIAN-VEHICLE INTERACTION AND CONTACT TIME AT 42 CM FROM THE VEHICLE CENTRELINE

| Impact Position	Vehicle Contact Region	Pedestrian Contact Region	Contact Time (ms)
Front	Front offset edge	Lower torso	0–43
	Front offset edge	Right femur	5-32
	Front edge and lower sheet plate	Right hand and arm	111-15
	Windscreen	Upper torso, specifically chest	12-47
	Front lower sheet plate	Right knee	17-32
	Upper side windscreen	Head	24-27
Rear	Front leading edge	Lower torso	0-27
	Front leading edge	Left arm	7-12
	Lower front sheet plate	Left knee	14-27
	Lower sheet plate	Left tibia	32-37
	Upper side corner of windscreen and frame	Head	60-65
Side	Right leading edge	Right arm	0
	Lower front sheet plate	Right hand	2-5
	Lower sheet plate	Right femur	47
	-	No torso contact	-
	-	No head contact	-
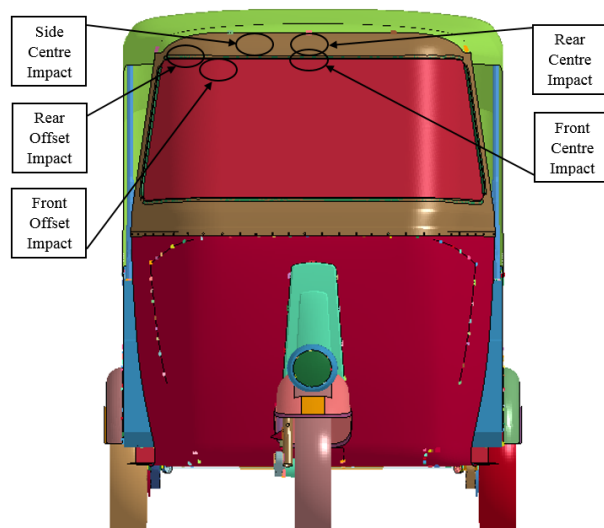
Fig. 5 Head contact locations of the auto rickshaw

TABLE X
HEAD CONTACT ANGLES DURING VARIOUS IMPACT POSITIONS

Impact Position	Head Impact Angles (Degrees)
Rear-centre	18
Rear-offset	47
Front-centre	31
Front-offset	24
Side-centre	45

During all of the impact simulations, though the head contact time was different for various impact positions and vehicle contact regions, the high velocity of collision resulted in short head contact times. No contacts occurred between the

head and vehicle components at 5 km/h during any collision scenario and side impacts appeared to be the safest for head

injury, since no head contacts occurred during the impact simulations, see Fig. 6.
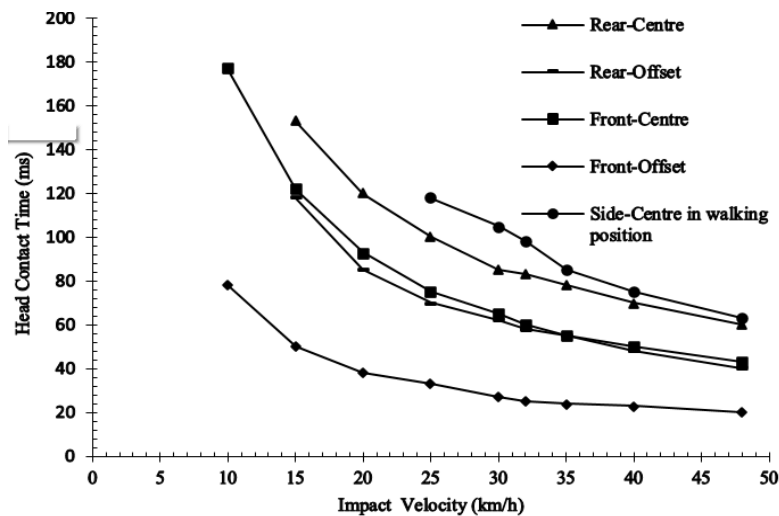

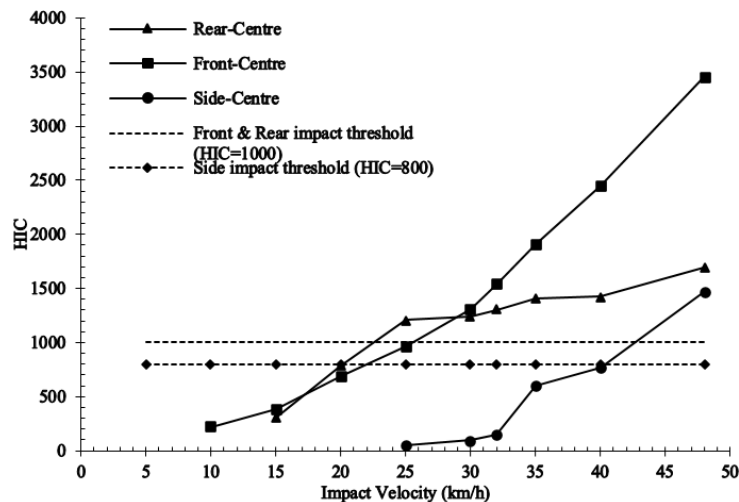Fig. 6 Head contact time at different impact positions

Fig. 7 HIC for impacts at the vehicle centreline at front, rear and side standing orientations

C. Head Injury and Injury Risk Level

1. Head Impact at the Centreline of the Vehicle

HIC for head impacts at different locations (front, rear and side) about the centreline of the vehicle are shown in Fig. 7. The HIC values increase significantly with vehicle impact velocity. For impacts to the front of the dummy, the HIC threshold (1000=HIC) was exceeded at 30 km/h. Whilst for rear impacts it exceeded the threshold (1000) at 2 km/h and for side impacts the threshold (800) was exceeded at 48 km/h.

The Association for the Advancement of Automotive Medicine (AAAM) specify the AIS for severe head injury as AIS+4, which corresponds with injuries including vault fractures, exposure or loss of brain tissue and small epidural or subdural haematomas [86]. To compare the effect of collision position, vehicle contact region and impact velocity on head

injury risk, a level of risk, corresponding with severe injury (AIS4+), was considered, based on the HIC for the adult pedestrian Hybrid III male dummy in collision with the auto rickshaw at impact velocities between 5 km/h and 48 km/h. Table XI, shows the probability of severe head injury increasing with increasing impact velocity.

Notably, an impact to the front at a velocity of 48 km/h corresponded with an almost 100% risk of an AIS+4 injury. For side impacts, the risk of severe head injury increased slightly between 25 km/h to 40 km/h, whilst increasing significantly at 48 km/h. Impacts to the rear corresponded with a steady increase in head injury risk.

2. Impacts at 42 cm Offset from Vehicle Centreline

HIC for head impacts at different locations (front, rear and side) offset at 42 cm from the centreline of the vehicle are

shown in Fig. 8. The HIC increased considerably with vehicle impact velocity. The HIC values are observed to have exceeded the frontal head impact threshold at 25 km/h and rear impacts at 20 km/h. Notably, there were no impacts to the side of the head during offset side impacts. For pedestrian impacts, at an offset of 42 cm from the vehicle centre, a correlation can be established between impact velocity and the percentage risk of severe head injury AIS+4, see Table XI. For frontal impacts, AIS+4 risk increased to 100% at 35 km/h, for rear impacts risk, it increased to 100% at 30 km/h and side impacts were absent. Therefore, the risk of sustaining a severe head injury (AIS+4) increased with increasing impact velocity. Moreover, the probability of an AIS+4 injury

depends on impact positions and vehicle contact region. Thus, it is clearly established that pedestrian impacts at velocities of 30 km/h or greater in the front offset position exceed the HIC threshold for risk of serious injury. In an attempt at deriving a simple solution to mitigating injury risk, Auto rickshaw windscreen thickness, which is 5.8 mm, was reduced to a thickness of 5 mm. From Fig. 9, it is clearly demonstrated that the 0.8 mm (13.8%) reduction in thickness produced only a 6.3% reduction in HIC and a corresponding reduction in resultant peak linear acceleration from 273 g to 250 g. Thus, confirming that injury risk remains high and cannot be mitigated simply by reducing windscreen thickness.
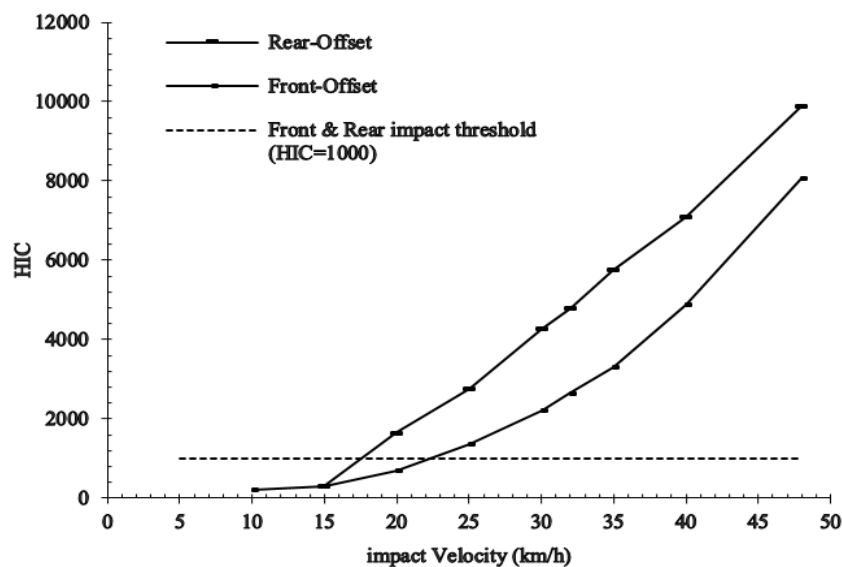

Fig. 8 HIC for impacts at a 42 cm offset from the vehicle centreline at two standing orientations
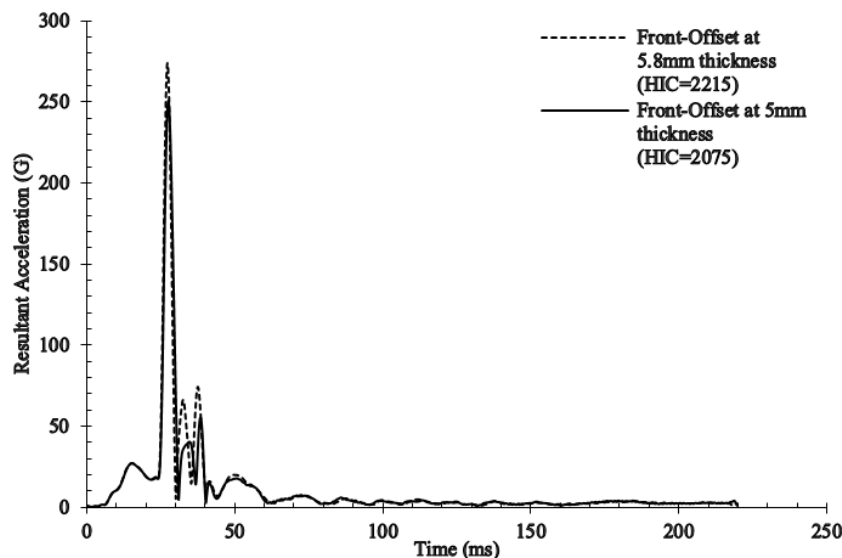

Fig. 9 Example of head acceleration curves for front 30 km/h offset impacts with two different windscreen thicknesses

Impact Velocity (km/h)	Rear-centre AIS+4%	Rear-offset AIS+4%	Front-centre AIS+4%	Front-offset AIS+4%	Side-centre AIS+4%
5	-	-	-	-	-
10	-	-	1.42	1.29	-
15	1.92	1.79	2.46	1.90	-
20	9.53	68.23*	6.91	6.92	-
25	31.43*	99.04*	16.27	43.78*	0.77
30	34.22*	100.00*	39.35*	94.02*	0.91
32	39.10*	100.00*	59.35*	98.64*	1.09
35	48.40*	100.00*	84.25*	99.86*	5.09
40	49.37*	100.00*	97.28*	100.00*	9.02
48	71.55*	100.00*	99.92*	100.00*	53.31*

*Probability of AIS+4 exceeds the threshold.

D. Upper Neck Injury and Injury Risk Level

1. Impacts at the Centreline of the Vehicle

Neck injury risk is represented by the Neck Injury Criterion, N_{ij} and N_{km} for the front and rear impact positions, respectively. For the front position, N_{ij} values were determined by selecting the worst case load condition, from each of the different collision velocities, see Fig. 10. The compression-extension (N_{ce}) was the worst case at 5 km/h and 10 km/h, respectively. Whilst tension-extension (N_{te}) has been selected as the worst possible load case, in terms of N_{ij}, at impact velocities between 15 km/h and 48km/h, for rear impacts, N_{km} values were identified by selecting the worst case load condition during each of the different collision velocities, see Fig. 11. The flexion-anterior (N_{fa}) was the worst case at 5 km/h and extension-posterior (N_{ep}) at 10 km/h. While, at 15 km/h, 20 km/h and 25 km/h, the flexion-posterior (N_{fp}) load case was the maximum peak between all of the upper neck load conditions and the flexion-anterior (N_{fa}) value was selected at 30 km/h as the worst case. Extension - anterior (N_{ea}) was the worst upper neck load case at 32 km/h. Finally, it appeared that the extension-posterior (N_{ep}) was the maximum load between 35 km/h and 48 km/h, see Fig. 11.
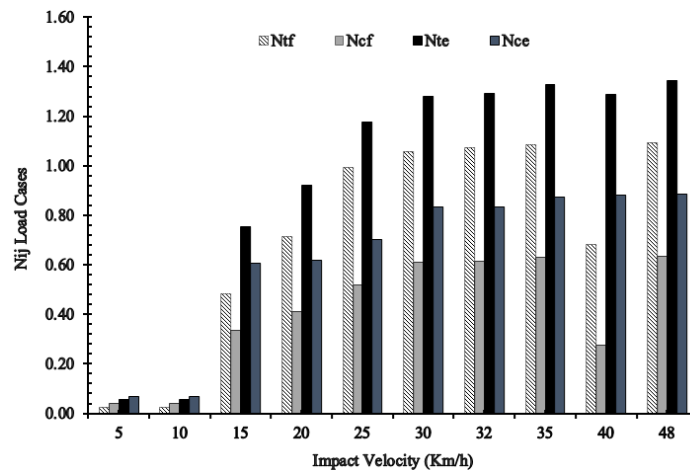

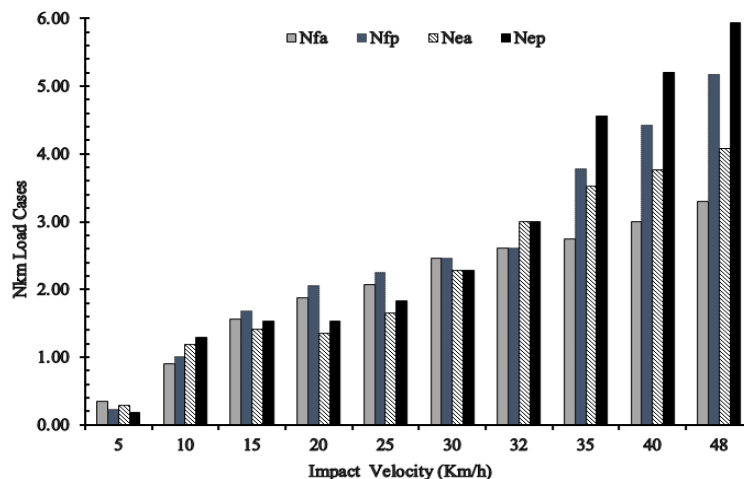Fig. 10 Upper neck load conditions for pedestrian impacts at the vehicle centreline (front position)

Fig. 11 Upper neck load conditions for pedestrian impacts at the vehicle centreline (rear position)

The maximum load conditions for the front and rear impacts (shown in Figs. 10 and 11) were selected to represent the worst case upper neck load situations, see Fig. 12. Both N_{ij} and N_{km} were observed to increase considerably with vehicle impact velocity. N_{ij} exceeded the frontal impact threshold at 25 km/h, and N_{km} exceeded the rear impact threshold at 10 km/h, which indicates a significantly greater upper neck injury vulnerability to rear impacts.

The influence of impact position, contact region and velocity on upper neck injury was investigated. Serious neck injury risk was assessed by relating N_{ij} and N_{km} to the AIS at a level of AIS3+, shown in Table XII. The risk of serious upper neck injury is seen to increase with impact velocity. An increasing neck injury risk from front impacts was in evidence between 5 km/h and 48 km/h, exceeding the threshold of 22% injury risk at 25 km/h. Rear impacts show a very significant increase in neck injury risk across the range of impact velocities exceeding the 22% injury risk threshold at 10 km/h and 100% risk at 35 km/h.

2. Impacts at 42 cm Offset from Vehicle Centreline

Impacts at a 42 cm offset from the vehicle centreline required consideration of both front (N_{ij}) and rear (N_{km}) impact loading of the neck. For front impacts (shown Fig. 13), the compression-extension (N_{ce}) worst case occurred at 5km/h, tension-extension (N_{te}) impacts in excess of 10 km/h and tension-flexion (N_{tf}) at 30 km/h and 40 km/h. For rear impacts (N_{km}), shown in Fig. 14, the flexion - posterior (N_{fp}) worst case was at 5 km/h, the flexion - anterior (N_{fa}) at 10 km/h, flexion - posterior (N_{fp}) between 15 km/h and 20 km/h and extension - posterior (N_{ep}) at 25 km/h to 48 km/h.
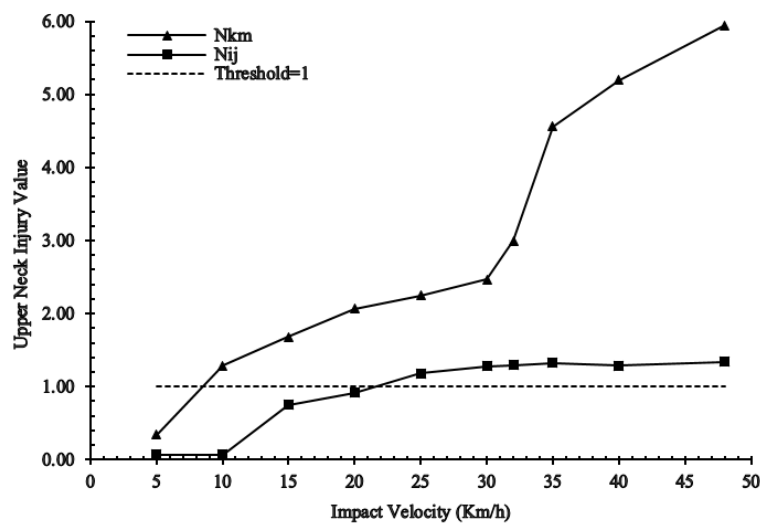

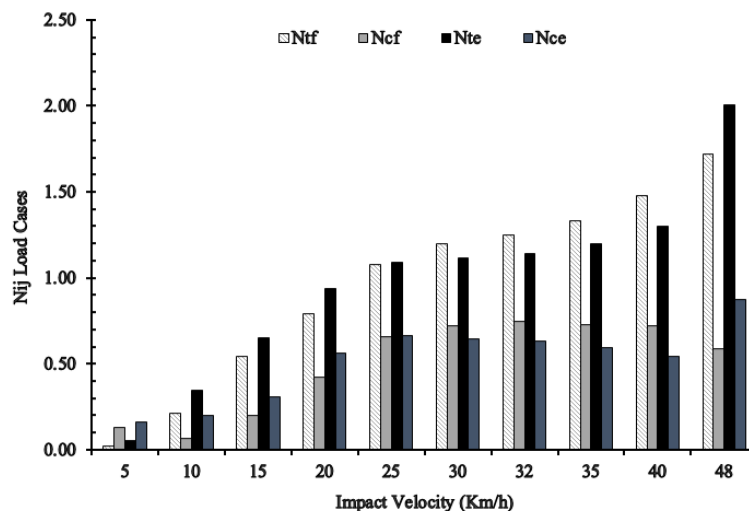Fig. 12 Upper neck injury values for pedestrian impacts at vehicle centreline (front and rear position)

Fig 13 Upper neck load conditions for pedestrian impacts at 42cm offset of vehicle centre (front position)
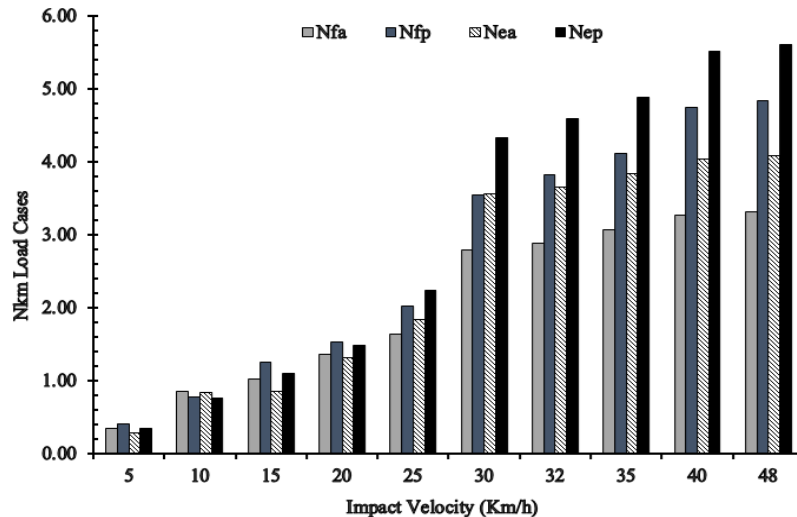
Fig. 14 Upper neck load conditions for pedestrian impacts at 42cm offset of vehicle centreline (rear position)
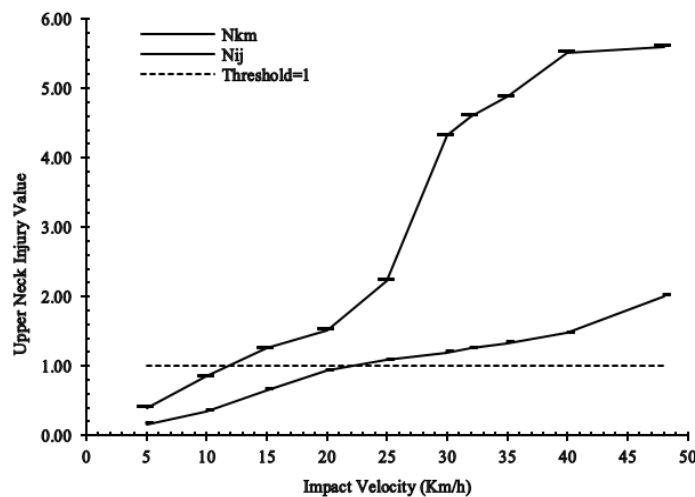

Fig. 15 Upper neck injury values for pedestrian impacts at 42 cm offset of the vehicle centre (front and rear position)

The worst load conditions for N_{ij} and N_{km} were chosen from Figs. 13 and 14, to represent the neck injury value and evaluate the risk of serious neck injury. Fig. 15 shows that both N_{ij} and N_{km} increased significantly with impact velocity. For frontal impacts, N_{ij} exceeded the threshold at 25 km/h; whilst for rear impacts, N_{km} exceeded the threshold at 15 km/h. Therefore, the rear impact position is considered the worst-case scenario with a high risk of severe neck injury, regardless of vehicle contact region (centreline or offset).

From Table XII, it can be seen that the risk of sustaining a serious neck injury increases with increasing impact velocity. Whilst the risk of injury from frontal impacts was observed to steadily increase with increasing impact velocities during rear impacts, a significant raise is seen in the probability of sustaining an AIS+3 level injury across all simulated impact velocities. Furthermore, the 22% injury threshold was exceeded at 15 km/h and the 100% threshold at 30 km/h.

TABLE XII
PROBABILITY OF SERIOUS UPPER NECK INJURY (AIS+3)

Impact Velocity (km/h)	Rear-centre AIS+3 (%)	Rear-offset AIS+3 (%)	Front-centre AIS+3 (%)	Front-offset AIS+3 (%)
5	7.24	8.04	4.34	5.16
10	33.23*	17.28	4.34	7.24
15	51.77*	31.83*	14.88	12.54
20	69.37*	44.19*	19.54	20.00
25	76.48*	76.24*	28.76*	25.25*
30	83.29*	99.50*	33.04*	29.55*
32	93.34*	99.70*	33.62*	31.82*
35	99.67*	99.83*	35.17*	35.37*
40	99.91*	99.95*	33.32*	42.03*
48	99.98*	99.96*	35.87*	67.30*

*Probability of AIS+3 exceeding the threshold.

IV. DISCUSSION

A. Pedestrian Kinematic Response

Real-world pedestrian impacts occur with highly variable

initial pedestrian kinematic and kinetic conditions. Small postural perturbations significantly influence vehicle impact kinematics and kinetics. This study investigated the kinematic response of an adult pedestrian, impacted by an auto rickshaw, subject to a narrow range of very specific initial conditions, since its objective was to computationally simulate the relatively unfamiliar impact biomechanics, compared to the common four-wheeled vehicles. The 50th percentile male Hybrid III was integrated with an auto rickshaw finite element model at a range of pre-impact velocities (5 km/h to 48 km/h). The influence of the pedestrian position during impact was investigated by varying three orientations (front, rear and side; relative to the vehicle) and two standing/gait postures, for a total of six simulated impact configurations. Pedestrian kinematics and injury risks were assessed and compared across all simulations.

In general, simulated frontal vehicle-pedestrian impacts produced high momentum transfer to the pedestrian in the forward direction as a result of contacts with the upper leg, hip and torso. With respect to the auto rickshaw, however, initial contact with the pedestrian occurred most frequently between regions of the lower limbs, significantly below the pedestrian's centre of gravity and the lower frontal vehicle parts (headlamp, mudguard and frontal sheet plate). This introduced many impact related kinematic perturbations, offset from the vehicle centreline, thus, influencing the subsequent dynamic response of the pedestrian.

With respect to subsequent direct impact between the front vehicle components and the pedestrian torso, impacts at the centreline prevented body rotation. Side impact to a walking posture produced rotation around the longitudinal axis, dependent on the forward or rearward position of the ipsilateral leg, since this created a lever arm and change in the orientation of the pelvis prior to impact [87]. Rear impacts produced momentum change principally at the lower and upper torso regions from contact with the lower parts of the windscreen and windscreen frame. Rear impact kinematic response was similar to the front impact in that little or no rotation was produced. The most significant post impact kinematic behaviour was rotation, when the dummy was impacted by the vehicle 42 cm offset from the centreline, due to impact asymmetry about the right and left side. In addition, side offset impact position produced imbalance and subsequent rotation around the longitudinal axis, as a result of three-wheel vehicle design, pedestrian mass, impact position with respect to the frontal side edge of the vehicle and walking posture, which generate a deceleration resistance 140 ms post impact, as shown in Fig. 4. In conclusion, the kinematic response of a pedestrian impacted by an auto rickshaw is most significantly influenced by pedestrian vehicle contact region, impact position and pedestrian posture, respectively.

B. Head Contact Locations, Angles, and Time

With respect to head impact, across all the vehicle pedestrian impact simulations, the most frequently impacted vehicle region was the windscreen and windscreen frame, see Fig. 5.

Changes in pedestrian impact position and vehicle contact region produced variations in head impact angles and head contact location; see Fig. 5 and Table X.

Head contact time was investigated at different impact velocities, with different impact positions and two vehicle contact regions (centreline and offset), see Fig. 6. Three pedestrian orientations were investigated for impacts at the centreline of the auto rickshaw. Front impacts produced no vehicle head impact at 5 km/h. Whilst, at velocities of 10 km/h, 20 km/h, 25 km/h, 30 km/h, 32 km/h, 35 km/h, 40 km/h and 48 km/h impact durations were produced as follows: 177 ms, 122 ms, 93 ms, 75 ms, 65 ms, 60 ms, 55 ms, 50 ms, 43 ms, respectively. For rear impacts, there were no head contacts at 5 km/h and 10 km/h. However, velocities of 15 km/h, 20 km/h, 25 km/h, 30 km/h, 32 km/h, 35 km/h, 40 km/h, 48 km/h produced impact durations of 153 ms, 120 ms, 100 ms, 85 ms, 83 ms, 78 ms, 70 ms and 60 ms, respectively. Side impacts produced no head impacts at 5 km/h, 10 km/h, 15 km/h and 20 km/h. However, at 25 km/h, 30 km/h, 32 km/h, 35 km/h, 40 km/h and 48 km/h head impact durations of 118 ms, 105 ms, 98 ms, 85 ms, 75 ms and 63 ms were produced, respectively. Front pedestrian impacts at 42 cm offset from the vehicle centreline produced no head contacts at 5 km/h. Impact velocities of 10 km/h, 15 km/h, 20 km/h, 25 km/h, 30 km/h, 32 km/h, 35 km/h, 40 km/h, and 48 km/h, produced head contact times of 78 ms, 50 ms, 38 ms, 33 ms, 27 ms, 25 ms, 25 ms, 23 ms and 20 ms, respectively, see Fig. 6. For rear impacts, no head contacts occurred at 5 km/h and 10 km/h. However, impact velocities of 15 km/h, 20 km/h, 30 km/h, 32 km/h, 35 km/h, 40 km/h and 48 km/h produced impact durations of 118 ms, 85 ms, 70 ms, 62 ms, 58 ms, 55 ms, 48 ms and 40 ms, respectively. Side impacts produced no head contacts across the range of impact velocities.

From Fig. 6, it can be seen that head contact time reduced with increasing impact velocity for all impact positions and vehicle contact regions as a result of increasing head accelerations. The simulation results show a close agreement with the data outlined in previous studies [3], [12], [88], [89]. Furthermore, the automotive designers can use these parameters to enhance active safety, such as pop up, Autonomous Braking Systems (ABS) and air bag technologies, considering the activation time protection with different pedestrian detection sensors [89]-[91].

C. Head Injury and Injury Risk Level

Changes in pedestrian impact position and vehicle contact region produced variations in head impact angles. HIC and head injury risk level varied considerably with impact position, vehicle contact region and impact velocity. Offset collisions produced the most dynamic impacts, with high HIC values being produced as a result of significant head kinematics prior to impact.

HIC values exceeding the injury risk threshold (HIC=1000 for front and rear impacts and 800 for side impacts) these thresholds correspond with an 18% risk of severe head injury (AIS+4) and are associated with bone structure deformation, soft tissue, skull fractures and brain contusions and lacerations

[63]-[68], [70], [92], [93].

HIC values were derived from the pedestrian impacts. For front centreline impacts, no head contact occurred at 5 km/h. Contacts were produced at 10 km/h and HIC values were observed to increase between 10 km/h, 15 km/h, 20 km/h, 25 km/h, 30 km/h, 32 km/h, 35 km/h, 40 km/h and 48 km/h to produce values of 222, 318, 689, 964, 1307, 1538, 1908, 2449 and 3450, respectively. The values exceed the head injury threshold, HIC=1000, between the velocities of 30 km/h and 48 km/h, shown in Fig. 7, corresponding with severe head injury (AIS+4) as shown in Table. XI. However, whilst HIC values are less than the injury threshold at 10 km/h, 15 km/h, 20 km/h and 25 km/h, they still represent a severe head injury risk, as shown in Table. XI. For rear impacts, no head contact occurred at 5 a km/h and 10 km/h; however, impacts at 15 km/h, 20 km/h, 25 km/h, 30 km/h, 32 km/h, 35 km/h, 40 km/h and 48 km/h, corresponded with HIC values of 309, 789, 1208, 1244, 13044, 1412, 1423 and 1693, respectively, as shown in Fig. 7. Therefore, the results emphasise that the HIC values exceed the threshold (HIC=1000) at 25 km/h or greater, as shown in Fig. 7. Corresponding with severe head injury (AIS+4), as illustrated in Table XI. HIC values, produced between 5 km/h and 20 km/h, whilst being less than the threshold, are still associated with head injury risk, as shown in Table XI.

For side impacts, no head contact was produced between 5 km/h and 20 km/h. The HIC values were low compared to front and rear impacts; though increased steadily. Impact velocities of 25 km/h, 30 km/h, 32 km/h, 35 km/h, 40 km/h and 45 km/h corresponded with values of 47, 95, 147, 597, 772 and 1468, respectively, as illustrated in Fig. 7. In addition, the percentage risk of sustaining severe head injury (AIS+4) was relatively small between 25 km/h and 40 km/h compared with front and rear impacts, as shown in Table. XI. Only at 48 km/h did the HIC value exceed the 800 threshold.

For 5 km/h, 42 cm offset frontal impacts; no HIC value was produced, since no head contact occurred. Impact velocities of 10 km/h, 15 km/h, 20 km/h, 25 km/h, 30 km/h, 32 km/h, 35 km/h, 40 km/h and 48 km/h produced HIC values of 195, 307, 690, 1359, 2215, 2650, 3311, 4884 and 8057, respectively. In addition, velocities between 25 km/h to 48 km/h h produced HIC values exceeding the 1000 threshold, shown in Fig. 8, corresponding with severe head injury (AIS+4), as shown in Table XI. Whilst the HIC values at 10 km/h, 15 km/h and 20 km/h are less than the injury threshold, they still represent a head injury risk, as shown in Table XI. For offset rear impact simulations, no HIC values were produced at 5 km/h and 10 km/h, though they increased significantly between 15 km/h and 48 km/h. Velocities of 15 km/h, 20 km/h, 25 km/h, 30 km/h, 32 km/h, 35 km/h, 40 km/h and 48 km/h produced values of 289, 1648, 2752, 4259, 4794, 5751, 7092 and 9878, respectively, as demonstrated in Fig. 8. Furthermore, the HIC value exceeded the 1000 threshold at 20 km/h and greater, shown in Fig. 8, severe head injury (AIS+4) is shown in Table. XI. The HIC value at 15 km/h, whilst not exceeding the injury threshold, is still associated with a head injury risk, as shown in Table. XI. For the side impact, no head injury was

observed, since no head impact was produced at any of the impact velocities. Therefore, the HIC and head injury risk level varied considerably with impact position, vehicle contact region and impact velocity. Offset collisions produced the most dynamic impacts, with high HIC values being produced as a result of significant head kinematics prior to impact.

The walking posture offset side impacts produced no head contacts with the vehicle, due to the significant pedestrian rotations, which were a result of asymmetry about the right and the left side of the dummy; while, an impact velocity below 20 km/h was associated with the lowest risk of severe head injury (AIS+4), less than 18%, as shown in Fig. 8 and Table XI.

D. Upper Neck and Injury Risk Level

The upper neck is a vulnerable region to injury, which is strongly associated with head movement. Upper neck injury risk is represented by the Neck Injury Criterion (N_{ij} and N_{km}), which is produced by considering the combination of force and moment, measured at the occipital condyles. Neck injury criterion (N_{ij} and N_{km}), is applied using neck injury thresholds, which is N_{ij} =1 and N_{km} =1, reported in [74], [77]. This indicates a 22% risk of serious neck injury (AIS+3) [74], which is associated with the rupture of small blood vessels of the occipital condylar joints, alar ligament rupture, damage to spinal cord (disc rupture and nerve root damage) and brainstem, and even death [74], [79], [80], [94]. Pedestrian impacts at the centreline of the vehicle were assessed for frontal impacts by the Neck Injury Criterion, N_{ij}., as shown in Fig. 10, which illustrated the upper neck load cases of the pedestrian impacts, calculated based on the combination of axial force and moment using (2). It appeared that the compression-extension load case (N_{ce}) represents the maximum load case of N_{ij} at both 5 km/h and 10 km/h, corresponding with 0.16 and 0.2, respectively. However, the tension-extension load case (N_{te}) represent the worst neck load with N_{ij} values, at 15 km/h, 20 km/h, 25 km/h, 30 km/h, 32 km/h, 35 km/h, 40 km/h and 48 km/h, of 0.65, 0.93, 1.09, 1.12, 1.14, 1.20, 1.30 and 2.01, respectively. The neck injury load cases (compression-flexion (N_{cf}) and tension-flexion (N_{tf})) have been excluded from the upper neck injury assessment of the front impact, since their values were lower than the worst-case injury cases ((N_{ce}), (N_{te})). The impact velocity exceeds the upper neck injury threshold (N_{ij}=1) at 25 km/h and greater, as shown in Fig. 12, and serious neck injury (AIS+3) is shown in Table XII, by using (5). Other neck injury values were lower than injury thresholds at 5 km/h, 10 km/h, 15 km/h, 20 km/h, though still represent a serious injury risk, see Table XII.

Rear impact related neck injury risk at the vehicle centreline was assessed by the Neck Injury Criterion, N_{km}, calculated based on the combination of shear force and moment using (3), as shown in Fig. 11. Flexion-anterior (N_{fa}) denotes the maximum load value of N_{km} at 5 km/h (0.35), which indicated a forward motion. Extension-posterior (N_{ep}) condition, indicated a rearward motion at 10km/h, with 1.29. However, the flexion-posterior (N_{fp}) condition, indicates the forward

motion, was maximal at 15 km/h, 20 km/h, and 25 km/h, corresponding with values of 1.68, 2.06, and 2.25, respectively. The flexion-anterior (N_{fa}) load condition indicated a forward motion at 30km/h corresponding with a value of 2.47. Extension-posterior (N_{ep}) load conditions produced the, highest risk upper neck load case, with a rearward motion at 32 km/h corresponding with a value of 2.99. Extension-posterior (N_{ep}), was a rearward motion at 35 km/h, 40 km/h and 48 km/h, producing values of 4.65, 5.20 and 5.94, respectively. Extension-anterior (N_{ea}) was excluded from the upper neck injury evaluation, since, it produced the lowest worst case ((N_{fa}), (N_{ep}), (N_{fp})). So, Velocities between 10 km/h and 48 km/h exceeded the upper neck injury threshold (N_{km}=1), see Fig. 12, corresponding to serious neck injury (AIS+3), shown in Table XII. A velocity of 5 km/h, whilst producing values less than the neck injury threshold, still represents a risk of serious neck injury, as shown in Table XII.

Neck injury risk for impacts at a 42 cm offset from the vehicle centreline was assessed by Neck Injury Criterion, N_{ij} for frontal impacts, as shown in Fig. 13. Calculated based on combination of axial force and moment, using (2) the worst case at 5 km/h was produced in compression-extension (N_{ce}) corresponding to a value of 0.16. Tension-extension (N_{te}) was the worst case neck load at 10 km/h, 15 km/h, 20 km/h, 25 km/h, 30 km/h, 32 km/h, 35 km/h, 40 km/h and 48 km/h producing an N_{ij} of 0.34, 0.65, 0.93, 1.09, 1.12, 1.14, 1.20, 1.30 and 2.01, respectively.

The neck injury load cases of tension-flexion (N_{tf}) and compression-flexion (N_{cf})) were disregarded from upper neck injury assessment for the front offset impacts, since the values were the lowest worst case injury risk ((N_{ce}), (N_{te})).

The impacts exceeded the upper neck injury threshold (N_{ij}=1) at 25 km/h or greater, as shown in Fig. 15 and serious neck injury (AIS+3), as shown in Table XII. Whilst the neck injury values at 5 km/h, 10 km/h, 15 km/h, and 20 km/h were less than the neck injury threshold, they still represent serious injury risk, as shown in Table XII.

Offset rear impacts, shown in Fig. 14, were evaluated, based on a combination of shear force and moment, using (3). Forward motion produced the greatest risk of injury during impacts at velocities between 5 km/h and 20 km/h. Flexion-posterior (N_{fp}) represents the worst risk of N_{km} at 5 km/h, corresponding with a value of 0.4. Whilst, flexion-anterior (N_{fa}) at 10 km/h corresponded with 0.84. The flexion-posterior (N_{fp}) showed the maximum upper neck load, when the impact occurred at velocities km/h between 15 km/h and 20 km/h, corresponding with 1.01 and 1.63, respectively. However, the extension-posterior (N_{ep}) provided the greatest risk of neck injury from a rearward motion at 25 km/h, 30 km/h, 32 km/h, 35 km/h, 40 km/h and 48 km/h corresponding with 2.23, 4.32, 4.88, 5.52 and 5.60, respectively. Extension-anterior (N_{ea}) was excluded from the neck injury assessment, since, it was mainly lower than other upper neck load cases. So, these results exceeded the upper neck injury threshold (N_{km}=1) between 15 km/h and 48 km/h, as shown in Fig. 15 and sustaining serious neck injury (AIS+3), as reported in Table XII. However, the

other neck injury values at 5 km/h and, 10 km/h were less than the neck injury threshold, although still represent injury risk, as shown in Table XII. Even when no head contact occurred, such as rear-centre impacts, high neck loading occurred corresponding with injury risk.

In terms of impact velocity for pedestrian impacts to the front (N_{ij}) and rear (N_{km}), increasing velocity produced increasing risk, as shown in Figs. 12 and 15, and Table XII.

With respect to pedestrian impact position, the values of the upper neck injury for rear impacts (N_{km}) were greater than upper neck injury values (N_{ij}) for frontal impacts at all impact vehicle velocities and contact regions (centreline and offset), as shown in Figs.12 and 15. Side impact related upper neck injury has not been investigated and is recommended for future work.

N_{km} calculation depends on the instantaneous shear force, which is produced by the vertical motion of the pedestrian spine pushing the head forward and then pulling the head backward, as shown in Fig. 4. The shear force (F_x) produces a high upper neck injury risk, compared to the axial force (F_z) acting during the front impact. Shear force is also associated with soft tissue injury to the intervertebral joints of the cervical spine, as specified in previous studies [95], [96].

Changing the vehicle contact region did not produce any significant influence on the N_{ij} value, exceeding the injury threshold at 25 km/h and greater, in the frontal impact (centreline and offset) as shown in Figs. 12 and 15. However, vehicle contact region did effect rear impact N_{km}, when it exceeded the threshold at 10 km/h and 15 km/h for the rear-centre and rear-offset impacts, as shown in Figs. 12 and 15. The simulation results in Figs. 7-15, demonstrate that the upper neck injuries will be more predominant than head injuries in some impact scenarios. What constitutes the safest impact velocity for upper neck injury may not be the same for head injury.

V. Conclusions

This study produced an improved understanding of pedestrian kinematics in auto rickshaw–pedestrian impacts, prior to head and neck impacts against the vehicle components. Key findings are summarised as follows:

1- Varying pedestrian impact position, pedestrian posture and vehicle contact region had a significant effect on the pedestrian kinematics and head contact angle.

2- Vehicle windscreen and windscreen frame are the most injury causative regions.

3- HIC and the percentage of severe head injury (AIS+4) values vary dependent on vehicle impact region, impact velocity and impact position. Pedestrians are subject to a relatively high risk of head injury at impact velocities of 20 km/h or greater.

4- The lowest risk impact scenario is the side offset, which produced no head contact.

5- Head and neck injuries can occur independent of each other. Even in the absence of a head impact, neck injury risk values were seen to exceed the threshold, as a result

of vehicle frontal geometry and pedestrian kinematics response.

6- Velocities below 10 km/h are associated with low neck injury risk.

To reduce the level of injury risk and increase the safety of the auto rickshaw, there should be a recommendation that the velocity of the auto rickshaw be reduced and that engineering solutions be developed, such as retro fitting injury mitigation technologies to those auto rickshaw contact regions, which are the subject of the greatest risk of producing pedestrian injury.

APPENDICES

TABLE XIII
DATA OF THE AXIAL FORCES AT DIFFERENT IMPACT VELOCITY USED TO CALCULATE THE NIJ OF THE FRONT-CENTRE

Velocity (km/h)	Tension (KN)	Time (ms)	Compression (KN)	Time (ms)
5	0.052	167	0.134	114
10	0.052	168	0.134	114
15	1.49	127	0.443	135
20	3.02	97.6	0.864	107
25	4.5	80.5	1.14	89.5
30	4.69	68.4	1.5	77.4
32	4.71	64.9	1.44	73.2
35	4.71	60	1.47	68.4
40	4.37	55.3	1.46	62.8
48	4.69	42.8	1.42	54.8

TABLE XIV
DATA OF THE BENDING MOMENTS AT DIFFERENT IMPACT VELOCITY USED TO CALCULATE THE NIJ OF THE FRONT-CENTRE

Velocity (km/h)	Flexion (KN.mm)	Time (ms)	Extension (KN.mm)	Time (ms)
5	5.13	65.3	6.31	129
10	5.13	65.1	6.31	128
15	82	134	72.1	149
20	83.9	106	64.3	119
25	103	88.4	69.8	103
30	114	77.1	79.8	92.3
32	118	72.5	81.2	88.4
35	122	67.6	85.9	82.1
40	12	60.8	87	76.8
48	125	46.7	88.4	70.4

TABLE XV
DATA OF THE AXIAL FORCES AT DIFFERENT IMPACT VELOCITY USED TO CALCULATE THE NIJ OF THE FRONT- OFFSET

Velocity (km/h)	Tension (KN)	Time (ms)	Compression (KN)	Time (ms)
5	0.0524	171	0.701	149
10	1.02	81	0.045	119
15	2.61	52.2	0.243	56.9
20	3.57	39.9	0.946	45.5
25	4.67	33	1.63	39.6
30	5.45	28.5	2	36.6
32	5.82	27.1	2.15	30.9
35	6.37	25.3	2.05	29.1
40	7.32	22.6	1.98	25.7
48	8.97	19.4	1.15	26.4

TABLE XVI
DATA OF THE BENDING MOMENTS AT DIFFERENT IMPACT VELOCITY USED TO CALCULATE THE NIJ OF THE FRONT- OFFSET

Velocity (km/h)	Flexion (KN.mm)	Time (ms)	Extension (KN.mm)	Time (ms)
5	5.13	65.3	6.31	129
10	18.5	84.5	26.2	99.5
15	49.1	58.7	36.3	42.8
20	83	46.3	55.4	36.1
25	122	39.3	54.2	30.4
30	123	33.6	42.9	26.5
32	123	31.8	38.4	24.4
35	123	29.7	35.2	49.5
40	124	25.8	30.2	43.8
48	125	22.3	92.8	38.6

TABLE XVII
NIJ LOAD CASES VALUES OF THE FRONT-CENTRE

Impact Velocity (km/h)	N_{tf}	N_{cf}	N_{te}	N_{ce}	N_{ij}
5	0.02	0.04	0.05	0.07	0.07
10	0.02	0.04	0.05	0.07	0.07
15	0.48	0.34	0.75	0.61	0.75
20	0.71	0.41	0.92	0.62	0.92
25	0.99	0.52	1.18	0.70	1.18
30	1.06	0.61	1.28	0.83	1.28
32	1.07	0.61	1.29	0.84	1.29
35	1.09	0.63	1.33	0.87	1.33
40	0.68	0.28	1.29	0.88	1.29
48	1.09	0.63	1.34	0.89	1.34

TABLE XVIII
NIJ LOAD CASES VALUES OF THE FRONT- OFFSET

Impact Velocity (km/h)	N_{tf}	N_{cf}	N_{te}	N_{ce}	N_{ij}
5	0.02	0.13	0.05	0.16	0.16
10	0.21	0.07	0.34	0.20	0.34
15	0.54	0.20	0.65	0.31	0.65
20	0.79	0.42	0.93	0.56	0.93
25	1.08	0.66	1.09	0.67	1.09
30	1.20	0.72	1.12	0.64	1.20
32	1.25	0.75	1.14	0.63	1.25
35	1.33	0.73	1.20	0.59	1.33
40	1.48	0.72	1.30	0.55	1.48
48	1.72	0.59	2.01	0.87	2.01

TABLE XIX
DATA OF THE SHEAR FORCES AT DIFFERENT IMPACT VELOCITY USED TO CALCULATE THE NKM OF THE REAR-CENTRE

Velocity (Km/h)	Anterior (KN)	Time (ms)	Posterior (KN)	Time (ms)
5	0.175	220	0.0817	50.3
10	0.318	133	0.409	113
15	0.47	93.7	0.573	75
20	0.527	73	0.679	57.7
25	0.595	62.1	0.739	46.5
30	0.904	53.1	0.902	40.6
32	1.03	50.7	1.03	38.2
35	1.14	59.7	2.02	70.5
40	1.35	43.9	2.56	64.2
48	1.61	47.2	3.19	57.3

TABLE XX
DATA OF THE BENDING MOMENTS AT DIFFERENT IMPACT VELOCITY USED TO CALCULATE THE NKM OF THE REAR-CENTRE

Velocity (km/h)	Flexion (KN.mm)	Time (ms)	Extension (KN.mm)	Time (ms)
5	12.2	68.5	4.07	44.2
10	46.7	130	38.3	153
15	88.5	93.4	40.4	112
20	111	74.4	34.9	94.9
25	121	63	45.3	82.1
30	123	54.1	57.9	82.1
32	123	51.6	84.3	78.2
35	123	48.8	103	71.4
40	123	44.4	103	65.4
48	123	39.3	103	58

TABLE XXII
DATA OF THE BENDING MOMENTS AT DIFFERENT IMPACT VELOCITY USED TO CALCULATE THE NKM OF THE REAR- OFFSET

Velocity (km/h)	Flexion (KN.mm)	Time (ms)	Extension (KN.mm)	Time (ms)
5	22.3	43	9.43	69
10	39.7	44.2	20.7	206
15	65.90	36.40	27.90	58.00
20	76.70	34.90	39.20	56.10
25	95.20	33.60	61.00	58.00
30	123.00	35.00	103.00	49.20
32	123.00	32.50	103.00	46.70
35	123.00	29.40	103.00	44.20
40	123.00	26.20	103.00	40.00
48	124.00	21.60	103.00	36.40

TABLE XXI
DATA OF THE SHEAR FORCES AT DIFFERENT IMPACT VELOCITY USED TO CALCULATE THE NKM OF THE REAR- OFFSET

Velocity (km/h)	Anterior (KN)	Time (ms)	Posterior (KN)	Time (ms)
5	0.0714	93.8	0.125	29.2
10	0.332	188	0.267	19.5
15	0.22	105.00	0.43	19.10
20	0.41	71.20	0.55	18.70
25	0.46	74.30	0.80	17.00
30	1.18	36.40	1.82	48.20
32	1.25	34.40	2.05	45.50
35	1.41	31.90	2.29	42.70
40	1.58	29.10	2.83	39.20
48	1.61	25.30	2.90	35.40

TABLE XXIII
NKM LOAD CASES VALUES OF THE REAR-CENTRE

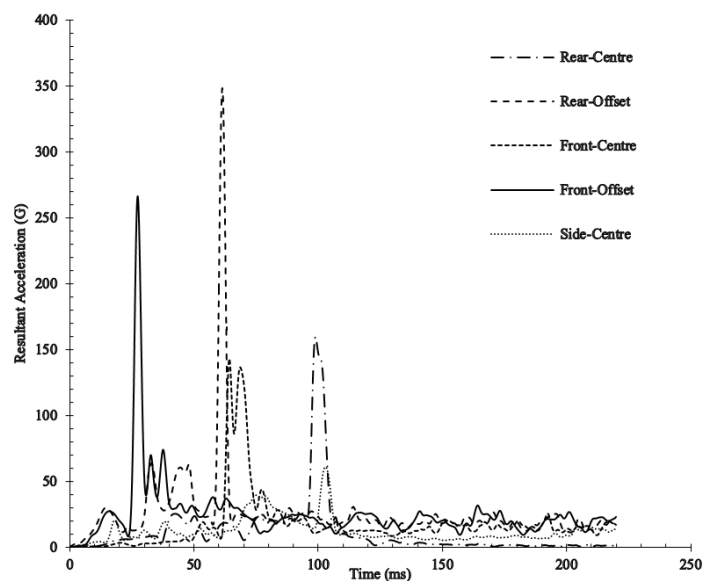| Impact Velocity (km/h)	N_{fa}	N_{fp}	N_{ne}	N_{np}	N_{km}
5	0.35	0.24	0.29	0.18	0.35
10	0.91	1.01	1.18	1.29	1.29
15	1.56	1.68	1.41	1.53	1.68
20	1.88	2.06	1.36	1.54	2.06
25	2.08	2.25	1.66	1.83	2.25
30	2.47	2.46	2.29	2.29	2.47
32	2.62	2.62	2.99	2.99	2.99
35	2.75	3.79	3.52	4.56	4.56
40	2.99	4.43	3.77	5.20	5.20
48	3.30	5.17	4.07	5.94	5.94

Fig. 16 Acceleration Curves of the pedestrian dummy head impacted at different impact positions and vehicle contact regions (30 km/h)

TABLE XXIV
NKM LOAD CASES VALUES OF THE REAR- OFFSET

Impact Velocity (km/h)	N_{fa}	N_{fp}	N_{ne}	N_{np}	N_{km}
5	0.34	0.40	0.28	0.35	0.40
10	0.84	0.77	0.83	0.75	0.84
15	1.01	1.25	0.85	1.09	1.25
20	1.36	1.52	1.31	1.47	1.52
25	1.63	2.03	1.83	2.23	2.23
30	2.79	3.55	3.56	4.32	4.32
32	2.88	3.82	3.65	4.59	4.59
35	3.06	4.11	3.84	4.88	4.88
40	3.27	4.75	4.04	5.52	5.52
48	3.31	4.84	4.07	5.60	5.60
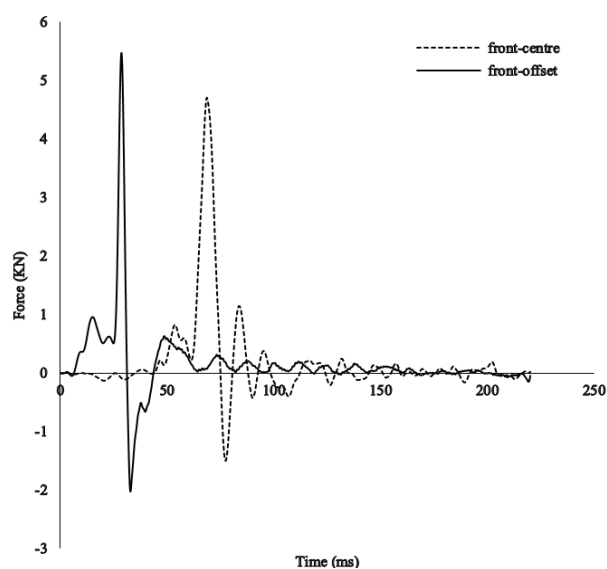
Fig. 17 Axial force of the Upper Neck at the Occipital Condyle in the Front Impact at (30 km/h)
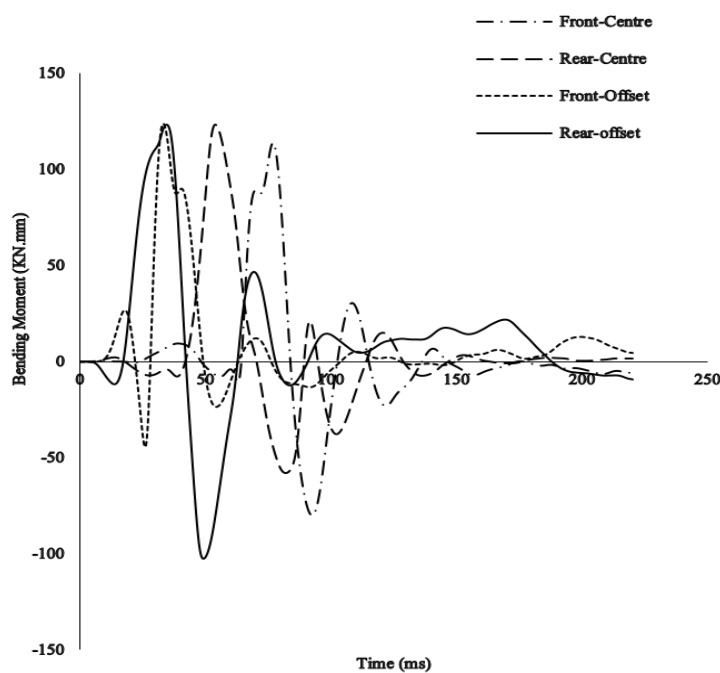

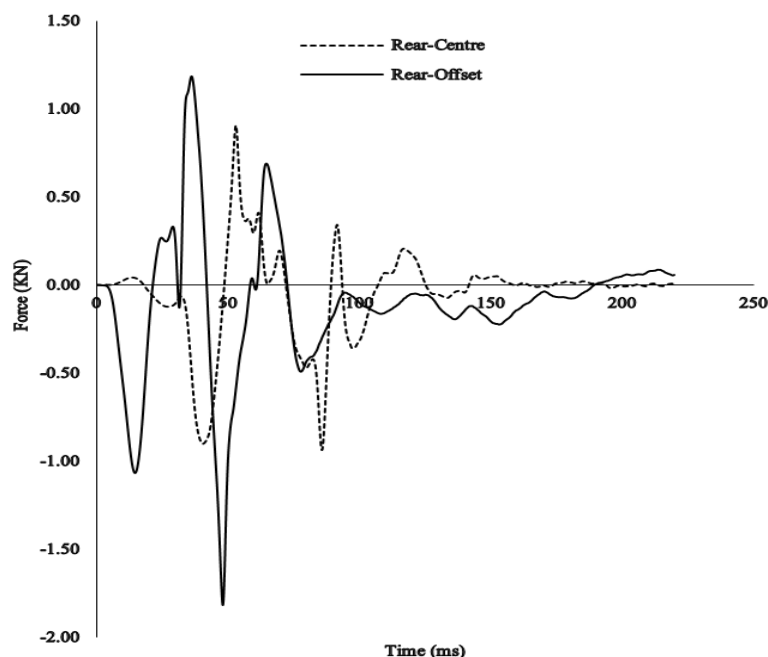Fig. 18 Bending Moment of the Upper Neck at Occipital Condyle at (30 km/h)

Fig. 19 Shear force of the Upper Neck at the Occipital Condyle in the Rear Impact at (30 km/h)

REFERENCES

[1] World Health Organization. WHO Global Status Report on Road Safety. Author; 2015. Available at: http://www.who.int/violence_injury_prevention/road_safety_status/2015/en/. Accessed June 2017.
[2] M. M. Hoque, M. McDonald, and R. D. Hall, "Road Safety Improvement in Developing Countries: Priority Issues and Options," in Proc. 20th Australian Road Research Board (ARRB) Conference, Melbourne, Victoria, Australia, 2001, pp. 1-15.
[3] Y. Han, J. Yang, K. Mizuno, and Y. Matsui, "Effects of Vehicle Impact Velocity, Vehicle Front-End Shapes on Pedestrian Injury Risk," Traffic Inj. Prev., vol. 13, no. 5, pp. 507–518, Feb. 2012.
[4] A. S. Al-Ghamdi, "Pedestrian–vehicle crashes and analytical techniques for stratified contingency tables", Accid Anal Prev., vol. 34, no. 2, pp. 205–214, March. 2002.
[5] W. Odero, P. Garner, and A. Zwi, "Road traffic injuries in developing countries: a comprehensive review of epidemiological studies", Trop. Med. Int. Health., vol. 2, no. 5, pp. 445–460. May. 1997.
[6] S. Sarkar, R. Tay, and J. D. Hunt, "Logistic Regression Model of Risk of Fatality in Vehicle–Pedestrian Crashes on National Highways in Bangladesh", Transportation Research Record No. 2264. Transportation Research Board of the National Academies, Washington D.C, pp. 128–137.
[7] J. R. Crandall, D. J. Lessley, J. R. Kerrigan, and B. J. Ivarsson, "Thoracic deformation response of pedestrians resulting from vehicle impact", Int J Crashworthiness., vol.1, no.6, pp. 529–539. Jul. 2006.
[8] Y. Han, J. K. Yang, K. Nishimoto, K. Mizuno, Y. Matsui, D. Nakane, S. Wanami, and M. Hitosugi, "Finite element analysis of kinematic behaviour and injuries to pedestrians in vehicle collisions". Int J Crashworthiness., vol. 17, no.2, pp. 141–152. April. 2012.
[9] J. R. Kerrigan, D. B. Murphy, D. C. Drinkwater, C. Y. Kam, D. Bose, and J. R. Crandall, "Kinematic corridors for PMHS tested in full-scale pedestrian impact tests," in proc. 19th International Technical of Conference on the Enhanced Safety of Vehicles (ESV), Lyon, France, 2005, Paper no. 05-0394, pp. 1-18.
[10] J. Kerrigan, C. Arregui, and J. Crandall, "Pedestrian head impact dynamics: comparison of dummy and PMHS in small sedan and lager SUV impacts," in proc. 21st International Technical Conference on the Enhanced Safety of Vehicles Conference (ESV), Stuttgart, Germany, 2009, pp. 1-15.
[11] X. Liu, and J. Wagner, "Design of a vibration isolation actuator for automotive seating systems—Part II: controller design and actuator performance". Int J Veh Des., vol. 29, no.4, pp. 357–375. January. 2002.
[12] X. Liu, and J. Yang, "Effects of vehicle impact velocity and front-end structure on dynamic responses of child pedestrians". Traffic Inj Prev., vol. 4, no.4, pp. 337–344. Jun. 2003.
[13] D. Longhitano, B. Henary, K. Bhalla, J. Ivarsson, and J. Crandall, "Influence of Vehicle Body Type on Pedestrian Injury Distribution," in proc. SAE, World Congress and Exhibition, 2005, SAE paper no. 1-1876.
[14] Y. Mizuno, and H. Ishikawa, "Summary of IHRA Pedestrian safety WG activities—proposed test methods to evaluate pedestrian protection afforded by passenger cars," in proc. 19th International Technical Conference on the Enhanced Safety of Vehicles(ESV), Washington, DC, 2005, pp. 1-15.
[15] C.D. Untaroiu, J. Shin, J. Ivarsson, J.R. Crandall, S. Damien, Y. Takahashi, A. Akiyama, and Y. Kikuchi, "A study of the pedestrian impact kinematics using finite element dummy models: the corridors and dimensional analysis scaling of upper-body trajectories". Int J Crashworthiness., vol.13, no.5, pp. 469–478. October. 2008.
[16] A. Mani, M. Pai, and R. Aggarwal, Sustainable Urban Transport Policy in India. INDIA, World resources institute, 2012.
[17] A. Garg, A. S. Gayen, P. Jena, G. S. Jose, L. Ramamurthy, K. M. Jiyad, and D. Dhanuraj, Study on the Auto rickshaw Sector in Chennai. INDIA, Civitas Consultancies Pvt Ltd for City Connect Foundation Chennai (CCCF), 2010, p. 220.
[18] http://lovson.com/lovson/three-wheeled-vehicles.html   (Online): (Accessed September 6, 2016).
[19] M. H. Mamun, M. Miah, and M. I. Islam, "Present Condition of Road Traffic Accident: A Case Study of Rajshahi City, Bangladesh," International Journal of Computer Applications. vol. 111, no. 7, pp. 975–8887. February. 2015.
[20] A. Mani, M. Pai, and R. Aggarwal, "Sustainable Urban Transport Policy in India: Focus on Auto rickshaw Sector," Journal of the Transportation Research Board, 2012.
[21] Government of India, Ministry of road transport and highways transport research, "Road Accidents in India-2015". Report, India, New Delhi, pp. 1–113. 2016.
[22] A. Jha, G. Tiwari, D. Mohan, S. Mukherjee, and S. Banerjee, "Analysis of Pedestrian Movement on Delhi Roads by Using Naturalistic Observation Techniques," Journal of the Transportation Research Board, 2017.
[23] D. Otte, "Severity and Mechanism of Head Impacts in Car to Pedestrian Accidents," in proc. International Research Council on Biomechanics of Injury (IRCOBI), Spain, 1999, pp.329-341.
[24] B. Fildes, H. C. Gabler, D. Otte, A. Linder, and L. Sparke, "Pedestrian

Impact Priorities Using Real-World CRASH Data and Harm," in proc. International Research Council on the Biomechanics of Impact (IRCOBI), Graz, Austria, 2004, pp.167-177.

[25] C. E. Neal-Sturgess, E. Carte, R. Hardy, R. Cuerden, L. Guerra, and J. Yang, "APROSYS European In-Depth Pedestrian Database," in proc. 20th International Technical Conference on the Enhanced Safety of Vehicles (ESV), Loyon, France, 2007, pp. 1–15.

[26] J. Louis Martin, A. Lardy, and B. Laumon, "Pedestrian Injury Patterns According to Car and Casualty Characteristics in France," in proc. 55th AAAM Annual Conference Annals of Advances in Automotive Medicine, vol.55, 2011. PP.137-146.

[27] L. Turner-Stokes, "The national service framework for long term conditions, a novel approach for a ''new style'' NSF". Journal of Neurology and Neurosurgery and Psychiatry. , vol. 76, no. 7, pp. 901-902. 2005.

[28] W. Liu, Z. Hui, K. Li, S. Su, X. Fan, Z. Yin, "Study on pedestrian thorax injury in vehicle-to-pedestrian collisions using finite element analysis". Chin. J. Traumatology., vol. 18, no. 2, pp. 74–80. April. 2015.

[29] J. K. Yang, "Review of injury biomechanics in car–pedestrian collisions". Int J Veh Saf., vol. 1, no. 1, pp. 100–116. 2005.

[30] [30] J. lous Martin, and D. Wu, "Pedestrian fatality and impact speed squared: Cloglog modelling from French national data". *Journal of Traffic Injury Prev*.2017

[31] R. W. G. Anderson, A. J. McLean, M. J. B. Farmer, B. H. Lee, and C. G. Brooks, "Vehicle travel speeds and the incidence of fatal pedestrian crashes". Accid Anal Prev., vol. 29, no. 5, pp. 667–674. September. 1997.

[32] S. J. Ashton. "A Preliminary Assessment of the Potential for Pedestrian Injury Reduction through Vehicle Design," in proc. 24th Stapp car crash conference, USA, 1980, SAE Paper 801315.

[33] S. J. Ashton, J. B. Pedder, G. M. Mackay, "Pedestrian Injuries and the Car Exterior," in proc. SAE Congress and Exposition, 1977, SAE Technical Paper 770092.

[34] R. Cuerden, D, Richards, and J. Hill, "Pedestrians and their survivability at different impact speeds," in Proc. 20th International Technical Conference on the Enhanced Safety of Vehicles (ESV), Washington, DC, USA, 2007, pp.1-12.

[35] L. Hannawald, and F. Kauer, Equal Effectiveness Study on Pedestrian Protection. Dresden, Germany. Technische Universität Dresden, 2004, pp.1-73

[36] C. Kong, and J. Yang, "Logistic regression analysis of pedestrian casualty risk in passenger vehicle collisions in China". Accid Anal Prev, vol. 42, no. 4, pp. 987–993. July. 2010.

[37] C. Oh, Y. S. Kang, and W. Kim, "Assessing the safety benefits of an advanced vehicular technology for protecting pedestrians". Accid Anal Prev. vol. 40, no. 3, pp. 935–942. May. 2008.

[38] E. Ros´en, U. Sander, "Pedestrian fatality risk as a function of car impact speed". Accid Anal Prev, vol. 41, no. 3, pp. 536–542. May. 2009.

[39] F. H. Waiz, M. Hoefliger, and W. Fehlmann, "Speed limit reduction from 60 to 50 km/h and pedestrian injuries," in Proc. 27th Stapp Car Crash and Child Injury and Restraint Conference With International Research Committee on the Bio kinematics of Impact (IRCOBI). 1983, pp. 277–285.

[40] S. J. Yaksich, Pedestrians with Mileage: A Study of Elderly Pedestrian Accidents in St. Petersburg Florida. American Automobile Association: Traffic Engineering and Safety Department, Washington, DC. 1964.

[41] Department for Transport, Speed: Know your limits. London, 2004.

[42] United Nations, Agreement Concerning the Establishing of Global Technical Regulations for Wheeled Vehicles, Equipment and Parts which can be Fitted and/or be Used on Wheeled Vehicles. Global technical regulation No. 9. Pedestrian Safety, 2008. (Available on line at: https://www.unece.org/trans/main/wp29/wp29wgs/wp29gen/wp29glob.html): (Accessed May 01, 2016).

[43] EEVC/CEVE, "The future for car safety in Europe," in proc. 5th International Technical Conference on the Enhanced Safety of Vehicles (ESV), London, 1974, PP.1-75.

[44] K. L. Jarrett, and R. A. Saul, "Pedestrian Injury - Analysis of the PCDS Field Collision Data," in proc. 16th International Technical Conference on the Enhanced Safety of Vehicles (ESV), Windsor, Ontario, Canada, 1998, pp. 1204–1211.

[45] C. B. Chidester, "Final Report-The Pedestrian Crash Data Study," in proc. 17th International Technical Conference on the Enhanced Safety of Vehicles (ESV), Amsterdam, the Netherlands, 2001.

[46] A. Noureddine, A. Eskandarian, and K. Digges, "Computer Modeling

and Validation of a Hybrid III Dummy for Crashworthiness Simulation". Journal of Mathematical and Computer Modelling, vol. 35, no. 7-8, pp. 885-893. 2002.

[47] http://www.dynaexamples.com/implicit/Yaris%20Dynamic%20Shock%20Absorber%20Loading, "LS-DYNA Examples." (Accessed November 10, 2016).

[48] L. A. Wood, N. Bekkedahl, and F. L. Roth, "Measurement of Densities of Synthetic Rubbers" Journal of Research of the National Bureau of Standards. vol. 29, no. 1939, pp. 391–396, 1942.

[49] K. M. Srikanth, and R. V. Prakash, "Assessing the structural crashworthiness of a three-wheeler passenger vehicle," in proc. 2nd International Conference on Research into Design, Bangalore, India, 2009, pp. 152–159.

[50] M. Haldimann, A. Luible, and M. Overened, Structural Use of Glass. Switzerland, Zürich: IABSE, AIPC and IVBH, 2008.

[51] C. Fors, Mechanical properties of interlayers in laminated glass Experimental and Numerical Evaluation. Lund University, 2014.

[52] S. Young Lee, "Crash-Induced Vibration and Safety Assessment of Breakaway-Type Post Structures Made of High Anticorrosion Steels". Journal of Shock and Vibration, vol. 2016, pp. 1-16, 2016.

[53] DMSB. Technical Regulations for DTM Vehicles. Deutscher Motor Sport Bund e.v, Frankfurt, 2015.

[54] G. James Group, G. James is glass. Brisbane, Australia, 2012.

[55] A. Livesey, and A, Robinson, the repair of vehicle bodies. New York: Routlede, 2013, ch. 4.

[56] http://es.euroncap.com/https://www.bajajauto.com/intracityvehicles/baja jre/ (Accessed accessed April 6, 2017).

[57] W. Liu, S. Su, J. Qiu, Y. Zhang, and Z. Yin, "Exploration of pedestrian head injuries-collision parameter relationships through a combination of retrospective analysis and finite element method," Int. J. Environ. Res. Public Health, vol. 13, no. 12, pp. 1–15, 2016.

[58] LS-DYNA, "What is the difference between *contact_automatic_single_surface and *contact_automatic_general?" 2016. (Online): (accessed Jan 10, 2017).

[59] J. Yang, "Effects of Vehicle Front Design Parameters on Pedestrian Head-Brain Injury Protection," in Proc. 18th International Technical Conference on the Enhanced Safety of Vehicles (ESV), Nagoya, Japan, 2003, pp. 1–8.

[60] R. Eppinger, E. Sun, S. Kuppa, and R. Saul, Supplement: Development of Improved Injury Criteria for the Assessment of Advanced Automotive Restraint Systems – II. National Highway Traffic Safety Administration, U.S. Department of Transportation, Washington, DC, 2000.

[61] G. Sarba, D. Bhalsd, and J. Krebs. LSTC Hybrid III dummies, positioning and post-processing. LSTC, Michigan, 2008, pp.1-21. (Available on line at: http://www.oasyssoftware.com/dyna/en/femodels/lstc_dummies/LSTC.H3.103008_v1.0_Documentation.pdf) (Accessed Sept 15, 2016).

[62] United Nations Economic Commission for Europe (UNECE). (Available online at https://www.unece.org/fileadmin/DAM/trans/doc/2004/wp29grsp/TRANS-WP29-GRSP-35-i...) (Accessed Oct 10, 2017).

[63] H. J. Mertz, P. Prasad, and G. Nusholtz, "Head Injury Risk Assessment for forehead Impacts," in proc. Congress and Exposition, SAE, 1996, PP. 1–23.

[64] United Nations, Proposed for a Global Technical Regulation on Uniform Provisions Concerning The Approval of Vehicles with Regard to their Construction in order to Improve The Protection and Mitigate the Severity of Injuries to Pedestrians and other Vulnerable Road Users, 2005. (Available at: https://www.unece.org/trans/main/wp29/wp29wgs/wp29grsp/grsp2005.html) (Accessed Feb 20, 2016).

[65] P. Prasad and H. J. Mertz, The Position of the United States Delegation to the ISO Working Group 6 on the Use of HIC in the Automotive Environment," in proc. Government Industry Meeting and Exposition, SAE, 1985, pp. 1–16.

[66] EEVC, "Improved test method to evaluate pedestrian protection afforded by pedestrian cars". Technical report, European Enhanced Vehicle Safety Committee, Working Group17, 2002, (Available at: https://www.unece.org/fileadmin/DAM/trans/doc/2006/wp29grsp/ps-187r1e.pdf) (Accessed accessed Nov 12, 2015).

[67] IHRA, Pedestrian safety working group, Technical Report, International Harmonized Research Activities, 2001.

[68] A. Kikuchi, K. Ono, and N. Nakamura, "Human Head Tolerance to Lateral Impact Deduced from Experimental Head Injuries Using Primates," in proc. 26th Stapp Car Crash Conference, SAE, 1982.

[69] E. Hertz, "A Note on the Head Injury Criterion (HIC) as a Predictor of the Risk of Skull Fracture," in Proc. 37th AAAM Conference, San Antonio, 1993.

[70] A. McIntosh, D. Kallieris, G. Krabbel, R. Mattern, N. Svensson and K. Ikels, "Head Impact Tolerance in Side Impacts," in proc. 15th International Technical Conference on the Enhanced Safety of Vehicles (ESV), Melbourne, Australia,1996.

[71] H. J. Mertz, and L. M. Patrick, "Strength and Response of the Human Neck," in Proc. 15th Stapp Car Crash Conference, SAE, 1971, Paper no.710855.

[72] H. Yamada, and G. Evans, Strength of Biological Materials. USA, Lippincott Williams and Wilkins, 1970, pp. 1-307.

[73] A. Sances, R. C. Weber, S. J. Larson, J. S. Cusick, J. B. Myklebust, and P. R. Walsh, "Bioengineering analysis of head and spine injuries," Journal of Critical Reviews in Bioengineering, vol. 5, no. 2, 1981, pp.79-122.

[74] R. Eppinger, E. Sun, F. Bandak, M. Haffner, N. Khaewpong, M. Maltese, S. Kuppa, T. Nguyen, E. Takhounts, R. Tannous, A. Zhang, and R. Saul, Development of Improved Injury Criteria for the Assessment of Advanced Automotive Restraint Systems – II. National Highway Traffic Safety Administration, U.S. Department of Transportation, Washington, DC, 1999.

[75] K. D. Klinich, R. A. Saul, G. Augste, S. Backaitis, and M. Kleinberger, Techniques for Developing Child dummy protection reference values. National Highway Traffic Safety Administration, USA, 1996.

[76] W. Goldsmith, and A. Ommaya, "Head and neck injury criteria and tolerance levels", in Chapon BA, (ed) Biomechanics of Impact Trauma, International Center for Transportation Studies. New York, Elsevier Science Publisher, 1984, pp 149–190.

[77] K.-U. Schmitt, M. H. Muser and P. Niederer, "A New Neck Injury Criterion Candidate for Rear-End Collisions Taking into account Shear Forces and Bending Moments," in proc. 17th International Technical Conference on the Enhanced Safety of Vehicles (ESV), Amsterdam, The Netherlands, 2001, pp. 1–9.

[78] T. Green, and T. Barth, "Injury evaluation and comparison of lateral impacts when using conventional and inflatable restraints," in proc. Creswell, OR: SAFE Association, 2006.

[79] M. J. C. Parr, M. E. Miller, N. R. Bridges, J. R. Buhrman, C. E. Perry, and N. L. Wright, "Evaluation of the Nij Neck Injury Criteria with Human Response Data for Use in Future Research on Helmet Mounted Display Mass Properties," in Proc. The Human Factors and Ergonomics Society 56th Annual Meeting, 2012, pp. 2070–2074.

[80] M. H. Muser, F. H. Walz, and H. Zellmer, "Biomechanical significance of the rebound phase in low speed rear end impacts.," in proc. International IRCOBI Conference on the Biomechanics of Impact, Montpellier, France, 2000, pp. 411–424.

[81] P. Susan, M. P. H. Baker, and B. O`Neill, "The Injury Severity Score," Journal of Trauma-Injury Infection & Critical Care, Vol. 16, no. 11, pp. 882–885. Nov. 1976.

[82] A. B. Chidester and R. A. Isenberg, "Final Report - The Pedestrian Crash Data Study," in Proc. 17th International Conference on the Enhanced Safety of Vehicles (ESV), Amsterdam, The Netherlands, 2001, pp.1-12.

[83] M. Richter, H. C. Pape, D. Otte, and C. Krettek, "Improvements in passive car safety led to decreased injury severity - A comparison between the 1970s and 1990s," Injury, vol. 36, no. 4, pp. 484–488. April. 2005.

[84] C. Arregui-Dalmases, M. C. Rebollo-Soria, D. Sanchez-Molina, J. Velazquez-Ameijide, and T. Alvarez, "Pedestrian head injury biomechanics and damage mechanism. Pedestrian protection automotive regulation assessment" Journal of Neurocirugia, vol. 28, no. 1, pp. 41–46. February. 2017.

[85] N. Yoganandan, F. A. Pintar, J. Zhang, T. A. Gennarelli, and N. Beuse, "Biomechanical Aspects of Blunt and Penentrating Head Injuries," IUTAM Symposium on Impact Biomechanics: From Fundamental Insights to Applications, 2005, vol. 124, pp. 173–184.

[86] T. A. Gennarelli, E. Wodzin. E, and AAAM, The Abbreviated Injury Scale 2005. Barrington, IL: American Association for the Advancement of Automotive Medicine, 2005.

[87] J. L. Forman, H. Joodaki, A. Forghani, P. Riley, V. Bollapragada, D. Lessley, B. Overby, S. Heltzel and J. Crandall, "Bio fidelity Corridors for Whole-Body Pedestrian Impact with a Generic Buck," in proc. International Research Council on the Biomechanics of Injury (IRCOBI), Lyon, France, 2015, pp. 356-372.

[88] X. J. Liu, J. K. Yang, and P. Lovsund, "A Study of Influences of Vehicle Speed and Front Structure on Pedestrian Impact Responses Using Mathematical Models," Journal of Traffic Injury Prevention, vol. 3, pp. 31-42, 2002.

[89] Y. Peng, C. Deck, J. Yang, D. Otte, and R. Willinger, "A study of kinematics of adult pedestrian and head impact conditions in case of passenger car collisions based on real world accident data", in proc. IRCOBI Conference, Dublin, Ireland, 2012, pp.766-778.

[90] E. Ros´en, J.E. Kallhammer, D. Eriksson, M. Nentwich, R. Fredriksson, and K. Smith, "Pedestrian injury mitigation by autonomous braking," Journal of Accid Anal Prev, vol. 42, 2010, pp.1949–1957.

[91] R. Fredriksson, E. Rosen, and A. Kullgren, "Priorities of pedestrian protection—a real-life study of severe injuries and car sources," Journal of Accid Anal Prev, vol. 42, pp. 1672–1681, 2010

[92] L. B. Cao, Z. Zhou, B. H. Jiang, and G. J. Zhang, "Development and validation of the FE model for a 10-year-old child head. Chin," Journal of Biomedical Engineering, vol. 33, pp. 63–70, 2014.

[93] S. Ruan, H. Li, X. Wang, and Y. Shen, "A New Exploration of the Applicability of the Head Injury Criterion," Journal of Biomedical Engineering., vol. 24, no.6, pp.1373-1377, 2007.

[94] R. Meijer, M. Philippens and J. van Hoof, "Side Impact Neck Injury Criteria and Tolerances in Aerospace Safety Injury", in proc. 13th International Workshop of Biomechanics Research, 2003, pp.31-46.

[95] K. H. Yang, P. C. Begeman, M. H. Muser, P. Niederer, F. Walz "On the role of cervical facet joints in rear end impact neck injury mechanism," SP-1226, SAE 970497, 1997, pp. 127-129.

[96] B. Deng, F. Luan, P. Begeman, K. Yang, A. King, S. Tashman, "Testing shear hypothesis of whiplash injury using experimental and analytical approaches," in Frontiers in Whiplash Trauma (Eds. N. Yoganandan and F. Pintar), IOS Press, Amsterdam 2000.

A. J. Al-Graitti received his B.E. degree in Mechanical Engineering from University of Baghdad in 2001 and his M.Sc degree in Municipalities Management from University of Baghdad in 2012. Currently he is a Ph.D. Student pursing Mechanical Engineering from Cardiff University, School of Engineering, Cardiff, UK.

G. A. Khalid received her Bachelor's degree in medical engineering from AL-Nahrain University, College of Engineering, Baghdad, Iraq in 2006, Master's degree in medical engineering from AL-Nahrain University in 2009, and Doctoral degree in medical engineering from Cardiff University, School of Engineering, Cardiff, UK, 2017. Her research interests are Biomechanics, Computational engineering, Head – Neck Injury& Prevention, Traumatic Brain Injury, Sport Medicine.

M. D. Jones is a Senior Lecturer in Clinical, Trauma and Orthopaedic Engineering at Cardiff School of Engineering, Cardiff University. His expertise is related to the biomechanical investigation of penetrative wounding and blunt force trauma, falls, playground accidents, non-accidental injury in children, including inertial injuries such as shaking. Dr. Jones is a member of The Chartered Society of Forensic Sciences.

R. Prabhu is currently an Assistant Professor in biomedical engineering in the Centre for Advanced Vehicular Systems (CAVS) and the Department of Agricultural and Biological Engineering (ABE) at Mississippi State University (MSU), Starkville, MS, USA. He leads MSU's research efforts in traumatic brain injury and multiscale modeling of biological materials. He obtained his Bachelor's degree in chemical engineering from the Indian Institute of Technology (IIT)-Madras, Chennai, India in 2000, Master's degree in computational engineering from MSU in 2005, and Doctoral degree in mechanical engineering from MSU in 2011.

P. Berthelson received his Bachelor's degree in Biological Engineering with a concentration in Biomedical Engineering from Mississippi State University, Starkville, MS, USA in 2016. He is currently pursuing a Master's degree in Biomedical Engineering from Mississippi State University, Starkville, MS, USA.